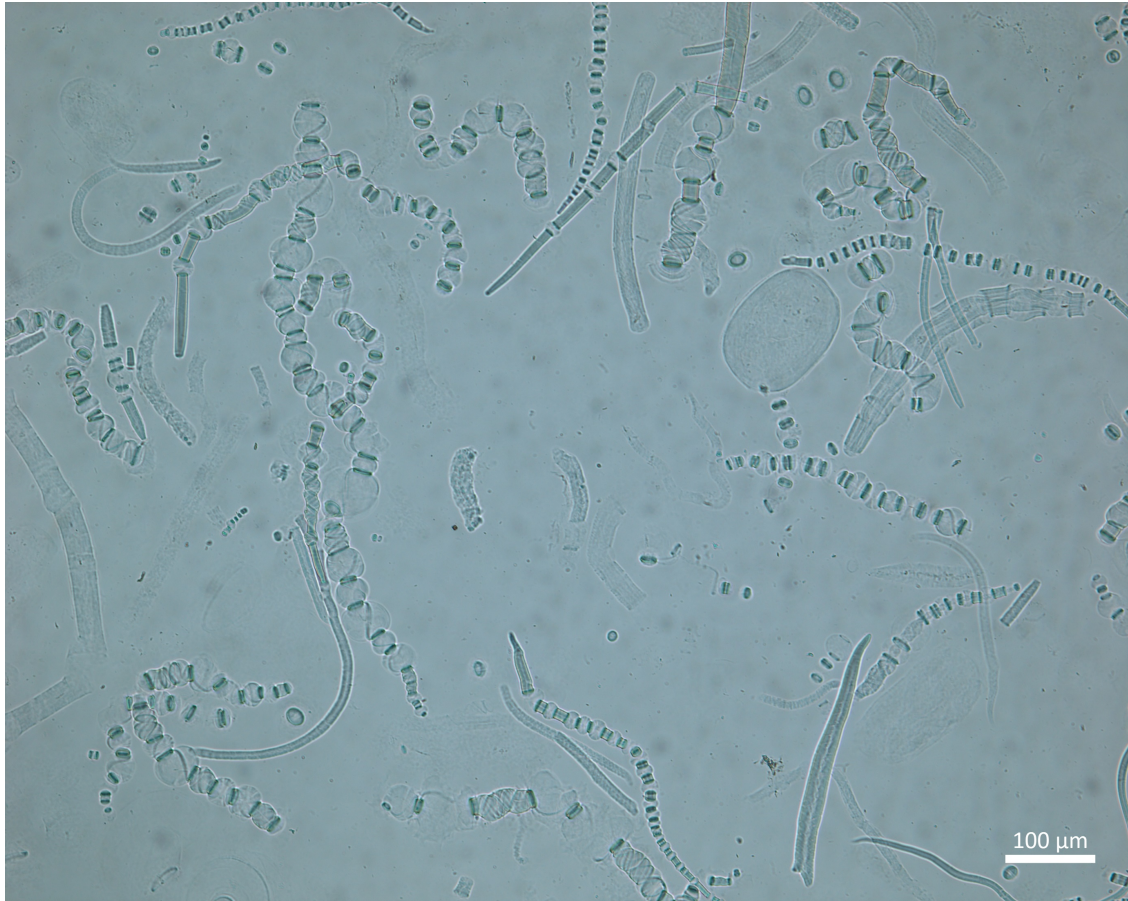




CHALMERS
UNIVERSITY OF TECHNOLOGY



Wheat Straw Cellulose Pulp

Production of dissolving-grade pulp using a combined organosolv–soda process for textile applications

Master's Thesis in Materials Chemistry

GABRIELLA COOPS

DEPARTMENT OF CHEMISTRY AND CHEMICAL ENGINEERING
CHALMERS UNIVERSITY OF TECHNOLOGY
Gothenburg, Sweden 2026
www.chalmers.se

MASTER'S THESIS 2026

Wheat Straw Cellulose Pulp
Production of dissolving-grade pulp using a combined
organosolv–soda process for textile applications

GABRIELLA COOPS



CHALMERS
UNIVERSITY OF TECHNOLOGY

Department of Chemistry and Chemical Engineering
Division of Applied Chemistry
CHALMERS UNIVERSITY OF TECHNOLOGY
Gothenburg, Sweden 2026

Wheat Straw Cellulose Pulp
Production of dissolving-grade pulp using a combined
organosolv–soda process for textile applications
GABRIELLA COOPS

© GABRIELLA COOPS, 2026.

Supervisor: Jenny Bengtsson, Department of Chemistry and Chemical Engineering at
Chalmers University of Technology and Maria Gunnarsson, TreeToTextile
Examiner: Diana Bernin, Department of Chemistry and Chemical Engineering at Chalmers
University of Technology

Master's Thesis 2026
Department of Chemistry and Chemical Engineering
Division of Applied Chemistry
Chalmers University of Technology
SE-412 96 Gothenburg
Sweden
Telephone +46 31 772 1000

Cover: Photograph showing swelled cellulose pulp in a cold alkali solution

Typeset in L^AT_EX
Gothenburg, Sweden 2026

Wheat Straw Cellulose Pulp
Production of dissolving-grade pulp using a combined
organosolv–soda process for textile applications
GABRIELLA COOPS
Department of Chemistry and Chemical Engineering
Chalmers University of Technology

Abstract

The demand for sustainable textile fibers has increased the interest in alternative cellulose sources instead of traditional wood-based pulp. This thesis studies the production and characterization of dissolving-grade cellulose pulp from wheat straw using a combined organosolv–soda pulping process. The aim was to evaluate if the produced pulp could be suitable for textile fiber production. This work was conducted in collaboration with Tree-ToTextile, reflecting an industrial interest in developing alternative cellulose feedstocks for fiber production.

Wheat straw was pretreated with ethanol/water mixtures containing 50% or 65% ethanol, with and without the addition of acid. After pretreatment, soda pulping was carried out using different effective alkali (EA) levels. Some samples also received an additional cold caustic extraction treatment. Grass was included as a second raw material to examine whether the process could be used for other annual plants. The produced pulps were analyzed based on chemical composition, intrinsic viscosity (IV), water retention value (WRV), color, and dissolution behavior in cold alkali (NaOH/ZnO).

The results showed that effective alkali was the dominant factor on cellulose chain length and dissolution behavior. Higher EA levels gave lower IV values and improved dissolution. Higher ethanol concentration and acid addition also improved lignin and hemicellulose removal. The highest cellulose purity was obtained with 65% ethanol at EA 0.72, while the highest glucose yield compared to the initial biomass was obtained with 65% ethanol at EA 0.48. For the samples with EA 0.48, IV had the strongest effect on dissolution, although cellulose purity and WRV also seemed to influence the results. The grass sample produced a cellulose-rich pulp with low lignin content under the same conditions as wheat straw. This shows that the process may also work for other annual plant materials.

Overall, the results showed that a mild organosolv–soda process can produce pulp with properties close to those needed for dissolving-grade applications from annual plant feedstocks.

Keywords: wheat straw, dissolving pulp, organosolv pretreatment, soda pulping, cellulose, textile fibers, annual plants

Acknowledgements

I would like to express my sincere gratitude to everyone who supported me during this master's thesis.

First, I would especially like to thank my supervisor at Chalmers, Jenny Bengtsson, who has helped me the most during this project. She has provided valuable guidance, support, and feedback throughout the work, both during planning and execution.

I would also like to thank my supervisor at the company, Maria Gunnarsson at TreeTo-Textile, for her continuous support, time, and practical input during the project. Her knowledge and advice were very helpful throughout the work.

I would like to express my thanks to my examiner, Diana Bernin, for her feedback and support during the thesis process.

I am also grateful to everyone else who contributed to the project through help, discussions, or practical assistance. Their input was very valuable.

Gabriella Coops, Gothenburg, June 2026

Contents

List of Figures	xi
List of Tables	xiii
1 Introduction	1
1.1 Background	1
1.2 Aim	3
1.3 Scope	3
2 Theory	4
2.1 Lignocellulose biomass	4
2.1.1 Wheat straw	4
2.1.2 Cellulose	5
2.1.3 Hemicelluloses	6
2.1.4 Lignin	6
2.1.5 Cell wall structure	7
2.2 Dissolving pulp	8
2.3 Processing annual plants into dissolving pulp	8
2.3.1 Organosolv pretreatment	9
2.3.2 Soda pulping	9
2.3.3 Cold caustic extraction	10
2.3.4 Hornification	10
2.4 Cellulose dissolution in NaOH/water	10
3 Methods	12
3.1 Raw material	12
3.2 Pretreatment	12
3.3 Soda pulping	12
3.4 Dry content	13
3.5 Cold caustic extraction	13
3.6 Dissolution	13
3.6.1 Aqueous NaOH–ZnO	13
3.6.2 EMIMAc	14
3.7 Analysis	14
3.7.1 Intrinsic viscosity (IV)	14
3.7.2 Compositional analysis	15
3.7.3 Microscopy analysis	15
3.7.4 Water retention value	16

3.7.5	Color measurement	16
4	Results and Discussion	17
4.1	Pulp composition	18
4.1.1	Effect of pretreatment solvent	18
4.1.2	Effect of acid concentration	20
4.1.3	Effect of extraction	23
4.1.4	Feedstock comparison	25
4.2	Pulp properties	26
4.2.1	Degree of polymerisation	26
4.2.2	Cellulose purity and intrinsic Viscosity	28
4.2.3	Mass yield and degree of polymerisation	29
4.2.4	Water retention value	31
4.3	Dissolution	33
4.4	Connecting pulp properties and dissolution	35
4.4.1	Dissolution and extraction	36
4.4.2	Dissolution and intrinsic viscosity	36
4.4.3	Cellulose purity and dissolution	37
4.5	Disclosure and declaration of AI use	39
5	Conclusion	40
6	Future work	41
	Bibliography	42
References		42
A	Appendix	I
A.1	Equations for pretreatment and pulping process	I
A.1.1	Dry content	I
A.1.2	Mass yield	I
A.1.3	Actual NaOH concentration	I
A.1.4	Actual L/S ratio	I
A.1.5	Water to add	I
A.2	Compositional data of samples	II
A.3	Brightness of samples	III
A.4	EMIMAc dissolution	IV
A.5	Equations - Intrinsic viscosity	IV

List of Figures

2.1	Cellulose molecules organised into microfibrils, macrofibrils, and cellulose fibers adapted from [13]	4
2.2	Wheat straw composition adapted from [14]	5
2.3	The molecular structure of cellulose adapted from [12]	5
2.4	Schematic diagram of the structure of wheat straw. Green lines represent cellulose fibers, orange lines represent hemicelluloses, and red dotted lines represent lignin. LCC=lignin-carbohydrate complex. Picture adapted from [14]	7
2.5	Phase diagram of the NaOH/H ₂ O/cellulose system adapted from [13]	11
4.1	Composition of total mass yield (wt%) after pretreatment with different concentration of ethanol/water.	19
4.2	Component yields from wheat straw (wt%) after pretreatment with different concentration of ethanol/water, expressed relative to initial biomass.	19
4.3	color difference (ΔE) between cellulose pulps and reference	20
4.4	Top row: pretreatment of cellulose without acid (left) and soda pulping (right). Bottom row: pretreatment with acid (left) and soda pulping (right)	21
4.5	Composition of recovered solids (wt%) after pretreatment with varying H ₂ SO ₄ concentrations in 50% ethanol/water and one sample with hot water and HCl.	22
4.6	Component yields from wheat straw (wt%) with varying H ₂ SO ₄ concentration in 50% ethanol/water pretreatment and one sample with hot water and HCl.	22
4.7	Color difference (ΔE) between cellulose pulps and reference	23
4.8	Effect of 1.5 wt% NaOH extraction on composition in total wt%. The values were not recalculated based on the recovered mass after extraction.	24
4.9	Color difference (ΔE) between cellulose pulps and reference	24
4.10	Composition of recovered material (wt%) for the grass sample and the wheat straw sample treated under the same conditions (50% ethanol, EA 0.48).	25
4.11	Color difference (ΔE) between cellulose pulp and reference for the grass sample and the wheat straw sample treated under the same conditions (50% ethanol, EA 0.48).	26
4.12	Relationship between cellulose purity (glucose/xylose ratio) and intrinsic viscosity (IV).	29
4.13	Relationship between mass yield (%) and intrinsic viscosity (IV) for EA 0.48 samples.	30
4.14	Relationship between mass yield (%) and WRV for EA 0.48 samples.	30

4.15	Relationship between mass yield (%) and cellulose purity (glucose/xylose ratio) for EA 0.48 samples.	31
4.16	Relationship between water retention value (WRV) and effective alkali (EA) for all samples.	33
4.17	Dissolution of 4% NaOH in 50% ethanol/water during thawing (12 L/S). Comparison between bright field and polarized light images.	33
4.18	Bright-field microscopy image showing fiber swelling (“ballooning”) during dissolution of pretreated cellulose in 4% NaOH (50% ethanol/water, EA 0.480).	34
4.19	Optical microscopy of the least effective dissolution condition (50% ethanol/water, EA 0.332). Polarized light images showing a high fraction of undissolved fiber.	35
4.20	Optical microscopy of the most effective dissolution condition (50% ethanol/water, 0.2% H ₂ SO ₄ , EA 0.960). Polarized light images showing improved fiber dissolution and reduced crystalline regions.	35
4.21	Relationship between intrinsic viscosity (IV) and undissolved in area% before and after 1.5 wt% NaOH extraction. Red points represent 50% ethanol samples at EA 0.48, green points represent EA 0.96. The white center indicate samples prior to extraction.	36
4.22	Relationship between intrinsic viscosity (IV) and undissolved in area%.	37
4.23	Relationship between cellulose purity (glucose/xylose ratio) and undissolved in area%.	39
A.1	Average L-value between cellulose pulps and reference	III
A.2	Colour distribution of cellulose samples in the A and B colour space. The red marker indicates the dissolution reference sample and the yellow marker indicate all the samples.	III
A.3	EMIMAc dissolution of the 50% ethanol sample with EA = 0.48.	IV

List of Tables

4.1	Pretreatment conditions and mass yield for wheat straw samples. All samples were treated at 175 °C for 2 h with a liquid-to-solid ratio of 12. . . .	17
4.2	Pretreatment conditions and mass yield for the grass sample. The sample was treated at 175 °C for 2 h with a liquid-to-solid ratio of 12.	18
4.3	Soda pulping conditions and mass yield for wheat straw samples. All samples were treated at 170 °C for 2 h and 25 min. EA refers to the effective alkali, expressed as g NaOH/100 g dry raw material.	18
4.4	Soda pulping conditions and mass yield for the grass sample. The sample was treated at 170 °C for 2 h and 25 min. EA refers to the effective alkali, expressed as g NaOH/100 g dry raw material.	18
4.5	Intrinsic viscosity (IV) for different cooking conditions grouped by treatment	28
4.6	WRV values for different cooking conditions grouped by treatment. . . .	32
A.1	Composition of wheat straw after pretreatment.	II
A.2	Composition of extracted wheat straw samples. With pretreatment condition of 50% ethanol/water	II
A.3	Composition of untreated wheat straw	II
A.4	Composition of grass sample after pretreatment	II

1. Introduction

1.1 Background

Textile consumption in the EU alone reached about 19 kg per person in 2022 [1]. Most textiles used in the EU are imported, and the textile industry ranks third in land use and water consumption [1]. It has also the fourth-largest negative impact on the environment and climate [2]. Globally, the fashion industry is regarded as the second most polluting industry after oil, leading to serious negative effects on the environment and society [3].

The textile industry has a major environmental impact at every stage of production. This includes the cultivation and extraction of raw materials, as well as the manufacturing processes used to spin fibers into yarns, weave fabrics, and apply chemical and finishing treatments. These processes use large amounts of water and energy, rely heavily on chemicals, and emit carbon emissions. The fast fashion business model has worsened these impacts by promoting frequent style changes and excessive consumption, as well as the use of low-quality synthetic fibers, which reduce the lifespan of clothes [4]. Globally, less than half of all discarded clothing is collected for reuse or recycling, and only 1% is recycled into new clothes [1].

Textile fibers can be natural or man-made fibers. Natural fibers are classified as plant-based, animal or mineral according to their origin and all three types are renewable, biodegradable, lightweight, strong, and mechanically recyclable. Today, most clothing materials are made from cotton or petroleum-based synthetic fibers. Cotton production requires large amounts of land, water, fertilizers, and pesticides, while synthetic fibers are made from fossil fuels and are not biodegradable. In addition, textile waste often contains blended fibers, especially mixtures of cotton and polyester, which makes recycling more difficult [4].

For this reason, there is increasing interest in cellulose-based fibers as more sustainable alternatives for the textile industry. Man-made fibers based on cellulose have been produced for over a century by dissolving and regenerating biomass. Using lignocellulose as a source of textile fibers could reduce dependence on oil and support a more sustainable textile industry [4].

Today, about 63% of the world's cellulose pulp comes from virgin wood fibers, 34% from waste paper, and only 3% from non-wood sources such as straw, bamboo, bagasse, reeds, grass, jute, flax, and sisal [5]. While wood is expected to remain important, its use is likely to expand into a wider range of applications in the future. In this context, since cotton production cannot easily be expanded, the increasing demand for cellulose-based textile

fibers may create a so-called "cellulose gap". This gap can partly be reduced through the use of man-made cellulosic fibers (MMCF), which can replace cotton in textile applications due to their similar functional properties. However, as MMCF production grows, competition for wood-based cellulose is expected to increase. Therefore, alternative cellulose sources such as agricultural side streams, referred to as next-generation fibers in the textile industry, are being explored as another strategy to address this challenge [5].

Cellulose from non-wood plants also offers several practical advantages. Many of these plants grow quickly and can often produce more material per unit area each year than trees. They are also often easier to process than wood because chipping and bark removal are usually not required. In addition, non-wood plants often contain less lignin than wood, which can make pulping easier and may reduce processing time, energy use, temperature requirements, and chemical consumption [5, 6].

Agricultural side streams, such as straw, leaves and husks can be used within a biorefinery concept, where multiple valuable components are extracted from the same raw material. The type and amount of side streams depend on geographical location, agricultural practices, and political regulations. However, practical and economic factors also need to be considered. These include how much material is available and when, how it can be collected and stored, and whether it competes with other industries [7]. To make agricultural side streams a viable raw material for cellulose extraction, certain requirements must be met. Dissolving-grade pulp requires a high α -cellulose content ($>90\%$) and low levels of hemicellulose ($<4\%$), lignin, and extractives [4]. If the cellulose content of the raw material is too low, or if the obtained pulp contains too many impurities such as hemicellulose, lignin, or extractives, the process may not be economically feasible. It is also important that cultivating plants specifically for textile fiber production does not compete with food crop production [8].

Wheat is one of the oldest and most widely cultivated crops in the world, and large amounts of wheat straw are produced every year as a by-product of wheat cultivation. Although wheat straw was previously considered agricultural waste, it is now seen as a valuable renewable resource for sustainable and bio-based applications. Wheat straw is a lignocellulosic biomass mainly composed of cellulose, hemicelluloses, and lignin. It also contains proteins, minerals, silica, and other bioactive compounds. Because of this composition, wheat straw can be used in several different processes. For example, the cellulose fraction can be used for bioethanol production, hemicelluloses for biohydrogen production, and the remaining waste for biogas production. This follows the biorefinery concept, where different parts of the same raw material are used efficiently to reduce waste. In addition, ash from agricultural residues has also been studied as a possible material in concrete production [9, 10].

TreeToTextile is a company that produces a new type of man-made cellulosic fiber for textiles and nonwoven materials. In their process, pure cellulose pulp is dissolved and converted into staple fibers through wet spinning. The resulting fiber can be used instead of cotton or viscose, either alone or blended with other fibers. At present, TreeToTextile uses cellulose from certified forestry [11]. However, as more industries move toward bio-based materials, competition for wood resources is expected to increase. Therefore, there is growing interest in finding other cellulose-rich raw materials that could reduce

dependence on wood and improve resource efficiency. This thesis focuses on alternative cellulose sources from agricultural side streams and evaluates wheat straw as a possible raw material for fiber production process.

1.2 Aim

The aim of this thesis was to produce and characterize dissolving-grade cellulose pulp from wheat straw using a combined organosolv–soda pulping method, and to evaluate whether the resulting pulp was suitable for textile fiber production.

1.3 Scope

Cellulose pulp was produced from wheat straw using a combined organosolv–soda pulping method. An additional alkaline extraction step was applied as a purification stage. The produced pulp was characterised in terms of molecular weight, chemical composition, and morphology.

Average molecular weight was determined by intrinsic viscosity measurements according to ISO standards commonly used in the pulping industry. Chemical composition was analysed through acid hydrolysis and liquid chromatography developed for carbohydrate analysis. The water retention value (WRV) was measured to evaluate the swelling behaviour and water uptake of the fibers.

The suitability of the pulp for textile fiber production was assessed through dissolution trials in cold alkali solvents and in the ionic liquid 1-ethyl-3-methylimidazolium acetate (EMIMAc). The resulting solutions were analysed using microscopy to evaluate the dissolution behaviour. In addition, the brightness of the pulp was determined.

The results from these analyses were used to evaluate the process conditions required to produce dissolving-grade cellulose suitable for textile applications.

This work does not include fiber spinning or the production of final textile materials.

2. Theory

2.1 Lignocellulose biomass

Lignocellulosic biomass, e.g. wood, straw, and grass, consists of three main polymers namely cellulose, hemicelluloses, and lignin, together with small amounts of other compounds such as proteins, ash, and pectin. Cellulose is embedded in a matrix of hemicelluloses and lignin, while covalent bonds mainly occur between lignin and hemicelluloses, and all three components are additionally connected through hydrogen bonds [4]. Cellulose has a partially ordered crystalline structure, whereas hemicelluloses and lignin are amorphous. Due to regular hydrogen bonds between cellulose chains, they organize into elementary fibrils containing alternating crystalline and amorphous regions [12]. The next larger structural unit, the microfibril, consists of bundles of elementary fibrils surrounded by hemicelluloses chains. These microfibrils then bundle together to form macrofibrils, with lignin and hemicelluloses filling the spaces between them, as seen in Figure 2.1 [13].

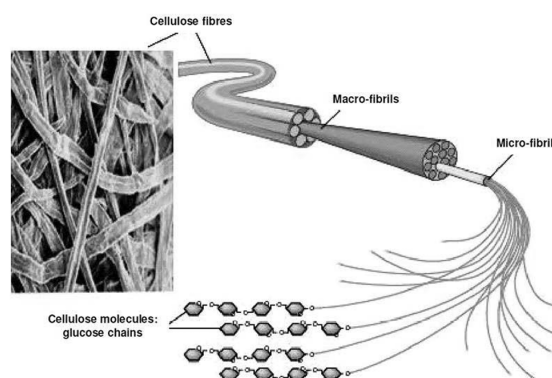


Figure 2.1: Cellulose molecules organised into microfibrils, macrofibrils, and cellulose fibers adapted from [13]

2.1.1 Wheat straw

A wheat plant has four main parts: the head, stem, leaves, and roots. The straw consists of the stem and leaves where the stem is divided into nodes and internodes, and the leaves consist of the leaf blade and leaf base, which can be seen in Figure 2.2. The chemical composition varies between these parts. The internodes are richest in carbohydrates (cellulose and hemicelluloses), the nodes have the highest lignin content, and the leaves and leaf bases contain the most ash, of which silica is the main component. Since the internode is the largest part of the straw, it is the most important fraction for cellulose extraction. The internode is hollow and surrounded by several layers. The outermost

layer, the epidermis, is rich in cellulose and silica [14, 15].

Between different biomass types, there are large differences in the amount of lignin and its specific chemistry. The chemical composition of wheat straw and wood varies not only with their origin but also with cultivar, soil type, fertilizer treatment, and other growth conditions. In general, wheat straw contains 11–26% lignin, 32–45% cellulose, and 20–45% hemicelluloses [10, 14].

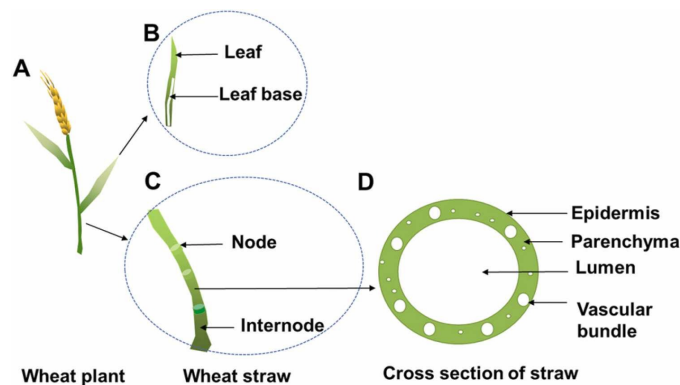


Figure 2.2: Wheat straw composition adapted from [14]

2.1.2 Cellulose

Cellulose is a linear polymer made of D-glucopyranose units (also called anhydroglucose units, AGUs) linked together by β -1,4-glycosidic bonds. Each AGU carries hydroxyl groups that form both intramolecular hydrogen bonds within the same chain and intermolecular hydrogen bonds between different chains. The intramolecular bonds affect the stiffness and shape of the chains, while intermolecular bonds help form larger structures such as crystalline domains and fibrils [4, 12]. Together, these hydrogen bonds, along with van der Waals and hydrophobic interactions, contribute to the insolubility of cellulose in water and most organic solvents [16].

The number of AGUs in a chain is referred to as the degree of polymerization (DP), which depends on the plant source and extraction method [12]. Although cellulose is sometimes described as a polymer of cellobiose, the repeating unit is glucose, since cellulose is formed by the successive addition of individual glucose residues [17]. The DP of cellulose varies depending on its origin and the method of isolation. Native cellulose from cotton has a DP of approximately 15 000, while wood cellulose has a DP of approximately 10 000 [18]. Regenerated cellulose fibers typically have a DP of 250–600 [13]. Shorter chains also occur, mainly in the primary cell wall. Each chain has two distinct ends: a reducing end (hemiacetal unit) and a non-reducing end with a hydroxyl group, as shown in Figure 2.3 [12].

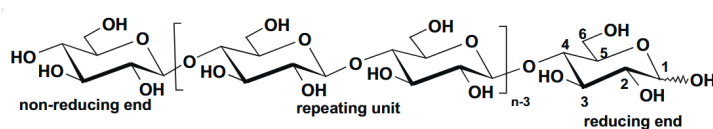


Figure 2.3: The molecular structure of cellulose adapted from [12]

Cellulose chains pack together into highly ordered elementary fibrils that bundle into microfibrils, giving cellulose its strength [4]. Less ordered amorphous regions within and between the microfibrils are more open and therefore more accessible to chemicals. In contrast, crystalline regions are tightly packed with strong hydrogen bonds that stabilize the structure. The type and structure of cellulose formed depend on the plant source, extraction method, and pretreatment used [12].

2.1.3 Hemicelluloses

Hemicelluloses are the second most abundant biopolymers in lignocellulosic materials after cellulose, making up about one third of total plant biomass. Unlike cellulose, hemicelluloses are heteropolysaccharides, meaning they are built from several different sugar units rather than just one, giving them a more complex and branched structure with a significantly lower degree of polymerization (DP 50-200) compared to native cellulose (DP ≥ 1000) [19].

Hemicelluloses form an amorphous matrix with lignin, in which cellulose microfibrils are integrated through hydrogen bonds and connected to other cell wall components through covalent bonds [4]. Together with cellulose, hemicelluloses help provide strength and flexibility to the cell wall. The type and amount of hemicelluloses in the cell wall vary depending on the plant species [4].

While xylan is the dominant hemicelluloses in hardwood and mannan in softwood, in grasses and cereal straws such as wheat straw, the dominant hemicellulose is arabinoxylan, which has a xylose backbone with arabinose side groups. Compared to wood xylans, wheat straw xylans have fewer uronic acids but more arabinose branches, making them particularly sensitive to acid hydrolysis [20, 21].

2.1.4 Lignin

Lignin is a complex three-dimensional polymer built from three types of building blocks: p-hydroxyphenyl (H), guaiacyl (G), and syringyl (S) units. These units are present in varying amounts depending on the plant species and even within the same species the lignin structure can vary significantly depending on growing conditions such as climate and nutrition. The units are connected by various ether and carbon-carbon bonds, which makes lignin difficult to fully break down [22, 23].

Lignin acts as a glue and structural support in the cell wall, filling the spaces between cellulose and hemicelluloses and surrounding the cellulose microfibrils together with hemicelluloses. It adds strength and rigidity to the cell wall and is more resistant to biological degradation than cellulose. Its strong cross-linking with cellulose also protects the cell wall against microbial and chemical attack [4]. Because lignin is covalently linked to both cellulose and hemicelluloses, removing lignin also leads to some degradation of carbohydrates [4].

During pulping, chromophoric structures form in lignin that give it a characteristic dark brown color. This colored lignin can adsorb onto fiber surfaces during processing, causing

staining and discoloration of the final pulp. The level of staining is directly related to the color intensity of the remaining lignin [24].

2.1.5 Cell wall structure

In the cell wall, cellulose chains pack together to form microfibrils. The arrangement and orientation of these microfibrils in each layer determines how the cell wall can deform and respond to stress. The microfibril orientation differs between wheat straw and wood. Both wood and wheat straw fibers consist of a middle lamella (ML), primary wall (P), and secondary wall (S). The middle lamella is a thin layer that glues neighboring cells together, and where three or four cells meet, this area is called the cell corner (CC). The secondary wall is further divided into three layers: the outer layer (S1), the middle layer (S2), and the inner layer (S3), as seen in Figure 2.4 [4, 14].

During pulp processing, the cell wall layers play different roles. The primary wall (P) acts as a barrier between the secondary wall and the outside, and must be broken to allow swelling and fibrillation. The S1 layer, which sits between the primary wall and S2, can limit the swelling of S2 and therefore also needs to be removed. The S2 layer is the main target of pulp processing, it is the thickest layer and makes up most of the fiber cell wall [25]. The S3 layer is generally not affected by pulp processing. In wheat straw, lignin is mainly connected to the arabinose side chains of xylan through ether bonds and since the middle lamella and cell corners make up a larger proportion of the cell wall in wheat straw than in wood, a higher percentage of the total lignin in wheat straw is located in these regions. This also means that removing xylan during pretreatment helps break the lignin network, further promoting delignification. [14].

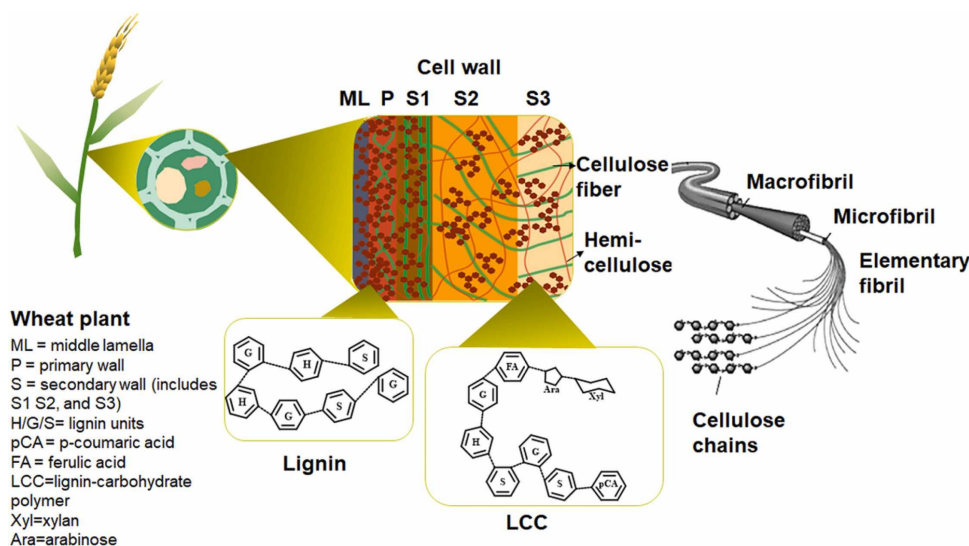


Figure 2.4: Schematic diagram of the structure of wheat straw. Green lines represent cellulose fibers, orange lines represent hemicelluloses, and red dotted lines represent lignin. LCC=lignin-carbohydrate complex. Picture adapted from [14]

2.2 Dissolving pulp

Cellulose is not thermoplastic and degrades before it melts, therefore it cannot be processed by melting like synthetic polymers such as polyester. Unlike synthetic fibers, which can be melted and extruded directly into fibers, cellulose must first be dissolved into a liquid phase and regenerated into a new fiber structure through wet-spinning. However, due to its well-defined structure, cellulose is barely accessible to any organic and inorganic solvents. Dissolution is therefore a necessary process step to transform the solid cellulose into a liquid phase from which it can be reformed into continuous filaments suitable for textile applications [13].

To enable dissolution, the cellulose pulp must therefore meet certain purity requirements, and pulp that fulfils these criteria is referred to as dissolving-grade pulp [13]. It consists of highly purified cellulose with an α -cellulose content above 90% and low levels of hemicelluloses, lignin, and extractives. Dissolving pulp should contain as little hemicelluloses as possible, since residual hemicelluloses on the fiber surface reduce the accessibility of cellulose to chemicals. Hemicelluloses are amorphous and highly sensitive to alkali, which increases solution viscosity and reduces diffusion into cellulose microfibrils, leading to less homogeneous alkali cellulose [4]. It can also decrease the mechanical strength of the final product and cause discoloration [4].

The degree of polymerization (DP) and carbohydrate composition are the two pulp properties with the most significant influence on solubility. Cellulose dissolution is therefore controlled by a complex interaction of both kinetic and thermodynamic factors [13]. Intrinsic viscosity, a measure of the average degree of polymerization of the cellulose chains, is commonly used to characterize dissolving pulp. The desirable intrinsic viscosity of dissolving pulp for viscose production is in the range 400–600 mL/g, and it is preferably reduced to 200–250 mL/g during production [26], whereas for the Lyocell process an intrinsic viscosity of 280–350 mL/g and a pulp DP of 650–750 is required [27]. An intrinsic viscosity that is too low may cause gel-like swelling of the viscose solution, making filtration difficult and negatively affecting the physical strength of the resulting fiber. An intrinsic viscosity that is too high will cause inhomogeneity [26].

2.3 Processing annual plants into dissolving pulp

Pretreatment is one of the key steps in processing lignocellulosic materials. Since cellulose, hemicelluloses, and lignin are strongly bound together in the plant cell wall, pretreatment is needed to break these bonds and make the cellulose more accessible. Chemical pretreatments aim to remove components that hinder cellulose accessibility, such as lignin and hemicelluloses, thereby increasing the cellulose concentration in the final pulp. However, the process can be limited by the complexity of the material, the presence of inhibitors, and the formation of unwanted byproducts [19].

Several pretreatment methods exist for breaking down the lignocellulosic matrix. Autohydrolysis uses only hot water in a pressurized reactor, without any added chemicals, to break down hemicelluloses into oligosaccharides. The process is driven by acids naturally released from the biomass itself, mainly acetic acid from hemicelluloses, which

catalyzes the hydrolysis [28]. Steam explosion involves placing the material under high pressure steam followed by a sudden decompression. This opens up the cell wall structure, degrades hemicelluloses and lignin, and increases cellulose accessibility [29]. Biological pulping uses microorganisms or enzymes to selectively break down lignin. While environmentally friendly and energy efficient, the process is slow and costly compared to chemical methods [5]. In the present work, organosolv pretreatment was used as the first processing step, as described in the following section.

2.3.1 Organosolv pretreatment

Organosolv pulping uses organic solvents as the cooking liquid to dissolve lignin and separate the fibers into pulp. The most commonly used solvents are organic alcohols such as ethanol, and organic acids such as formic acid and acetic acid. Other options include esters, phenols, and solvent mixtures. A key advantage of this approach is that the solvents can be easily recovered by distillation. When used without acid catalysts, the process is also sulfur- and chlorine-free, replacing inorganic chemicals with more environmentally friendly alternatives [5, 30].

Organosolv pretreatment can also be combined with a small amount of acid catalyst such as sulfuric acid to enhance both delignification and hemicelluloses hydrolysis, though this reduces the sulfur-free advantage of the process. Because glycosidic bonds in hemicelluloses are acid-sensitive, the addition of acid promotes hemicelluloses removal, while the organic solvent dissolves and extracts the lignin [19, 31].

Organic solvents such as ethanol serve two functions: breaking the bonds between lignin and hemicelluloses as well as ether bonds in lignin, and dissolving the lignin fragments to prevent them from repolymerizing. The combination of ethanol and sulfuric acid therefore targets both lignin removal and hemicelluloses dissolution, resulting in a cellulose-rich solid fraction with increased accessibility [32].

2.3.2 Soda pulping

Soda pulping is a chemical process used to remove lignin from biomass using sodium hydroxide (NaOH). Delignification occurs by breaking bonds in the lignin structure, which can also lead to some loss of carbohydrates. This process does not use sodium sulfide, so the lignin produced is sulfur-free and less chemically modified than kraft lignin. However, it is still different from natural lignin. Cellulose is more resistant to alkaline conditions and breaks down less than hemicelluloses [12, 33].

During soda pulping, alkaline conditions efficiently remove and depolymerize lignin, which dissolves in the cooking liquid and can be isolated. The bonds between lignin and hemicelluloses are also cleaved, further altering the lignin structure [14].

An alkaline side stream called black liquor is produced during pulping, containing dissolved lignin and spent cooking chemicals. Black liquor from wheat straw is more problematic than from wood due to its higher silicon and potassium content, which causes deposits in recovery boilers and corrosion. However, silica can be selectively removed from the black liquor and recovered as a valuable by-product [34].

2.3.3 Cold caustic extraction

Cold caustic extraction (CCE) is a method for removing hemicelluloses from cellulose pulp using a cold alkali solution. Dissolving pulp requires a very low hemicelluloses content, which standard pulping alone often cannot achieve, making CCE a useful additional treatment. CCE works by swelling the cellulose fibers in an alkaline solution, which allows the hemicelluloses to dissolve and be removed. It selectively removes hemicelluloses, which also increases the degree of polymerization of the remaining cellulose. Furthermore, CCE improves dissolution by reducing the DP and changing the carbohydrate composition of the pulp, thereby increasing the stability of the cellulose solution. When cellulose comes into contact with the alkali solution, the amorphous regions swell and alkali ions penetrate into the crystalline regions, forming alkali cellulose, which has a more open and reactive structure compared to native cellulose [35, 13].

A key advantage of CCE is that the extracted hemicelluloses, especially xylan, is obtained in its polymeric form, making it potentially valuable for other applications. CCE also produces pulp with higher alpha-cellulose content and a narrower molecular weight distribution. However, a key drawback is that high NaOH concentrations can convert cellulose I to cellulose II, which has implications for dissolution [35, 36].

2.3.4 Hornification

Hornification is a process in which cellulose fibers irreversibly lose their porosity as water is removed. When water leaves the cell walls, pores collapse and fibrils stick together, causing the internal fiber volume to shrink. Once dried fibers are resuspended in water, they do not fully regain their original swollen state. Hornification reduces cellulose reactivity by closing pores that would otherwise be accessible to solvents, and generally increases with higher drying or processing temperatures, though the relationship has been shown to be condition-dependent [37, 38].

During chemical pulping, the removal of lignin and hemicelluloses generates large pores that collapse upon drying, causing elementary fibrils to aggregate into larger structures called macrofibrils. Hornification begins as soon as cell wall polymers are removed and is worsened by processes that shear, compress, or dry the fibers [39].

To improve cellulose reactivity and dissolution, various activation methods are used that aim to increase porosity, reduce the degree of polymerization, and remove non-cellulosic components such as hemicelluloses and lignin. The outermost layers of the cell wall, specifically the primary wall and the S1 layer, are the most difficult to dissolve. Activation methods therefore aim to partially or fully remove these outer layers to promote more even dissolution [25].

2.4 Cellulose dissolution in NaOH/water

Cellulose is considered difficult to dissolve for two main reasons. First, cellulose chains are very rigid, which limits their freedom of movement when entering a solvent [29]. Second, cellulose has an amphiphilic character, with both polar and nonpolar regions. Although hydrogen bonds have traditionally been considered the main cause of cellulose

insolubility, it has been shown that hydrophobic interactions, van der Waals forces, and the rigid chain structure all contribute to its resistance to dissolution [40]. Beyond these thermodynamic challenges, dissolution also has a kinetic aspect, meaning it is not just about whether dissolution is possible, but also how fast it occurs. This is why cellulose often needs to be activated before dissolution, through methods that help the fibers swell and become more accessible to the solvent [29].

When cellulose comes into contact with a strong alkali solution, its structure starts to change. The amorphous regions between the fibrils are the first to swell, and the alkali ions then penetrate further into the more crystalline regions. At certain concentrations intermediates called alkali cellulose are formed, which have a more open and reactive structure compared to native cellulose. There are five forms of alkali cellulose (Na-Cell I, II, III, IV, and V), each forming at different temperatures and NaOH concentrations. Interestingly, below 0°C and below 10 wt% NaOH, shown as the area Q in Figure 2.5 [13], cellulose dissolves.

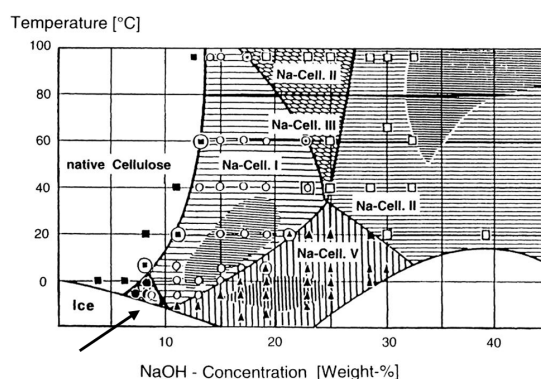


Figure 2.5: Phase diagram of the NaOH/H₂O/cellulose system adapted from [13]

The dissolution mechanism for cellulose in NaOH has been studied intensively [29]. At very low concentrations, it has been suggested that the hydrated ions are too large to effectively penetrate between cellulose chains, although several competing explanations exist. As concentration increases, the ions become less strongly hydrated and are able to penetrate into the amorphous and then crystalline regions. However, if the concentration is too high, the ions cannot effectively break hydrogen bonds in cellulose, limiting dissolution. Aqueous cellulose–NaOH solutions are also unstable and tend to gel over time, with gelation accelerating at higher temperatures. Mixing and processing should therefore be performed below 0°C [29].

The dissolution mechanism for cellulose depends mainly on solvent quality, but also on the morphology of the fiber, specifically whether the primary wall is still intact [29]. When natural cellulose fibers are placed in a less good solvent, such as NaOH(aq), they do not swell evenly. Instead, swelling occurs only in certain zones along the fiber, creating a phenomenon known as ballooning. The swelling of the secondary wall causes the primary wall to stretch and burst, and the swollen cellulose pushes through tears in the primary wall, which then rolls up to form collars, rings, or spirals that restrict uniform expansion and create balloon-like structures [29].

3. Methods

3.1 Raw material

Wheat straw was supplied by a farmer from Skåne, Sweden, and the grass was supplied from Schleswig-Holstein, Germany. The dry content of the raw materials was measured to 90% prior to cooking. Therefore, 55 g of raw material was weighed out per batch to obtain a dry weight of 50 g, with an allowable margin of ± 0.01 g.

3.2 Pretreatment

The experiments were carried out in 1.2 L steel autoclaves equipped with screw-on locks, which were heated in a temperature-controlled polyethylene glycol bath (PEG 400, 270 L) with external ventilation.

Solutions with a liquid-to-solid (L/S) ratio of 12 were prepared using either water, ethanol, sulfuric acid, or hydrochloric acid, as specified in Tables 4.1 and 4.2. The solutions and raw material were then added to the autoclaves. The autoclaves were placed in a pre-heated polyethylene glycol bath at 175 °C for 2 hours, after which they were cooled in a cold water bath.

A Büchner funnel with a woven polypropylene mesh (200 μm) was placed on top of an Erlenmeyer flask. The pulp from the autoclaves was poured into the funnel and separated by filtration, with the flask connected to a vacuum line to speed up the process. The autoclaves were then rinsed with water, and the rinsing water was added to the funnel to recover any remaining solid material. The pretreated straw was repeatedly washed with water until colorless faded and the pH of the remaining liquid was neutral, as measured with pH strips.

3.3 Soda pulping

Solutions of NaOH in water with different concentrations were prepared based on the liquid-to-solid (L/S) ratio: 8.3 or 12. First, the pretreated wet solids were weighed. The dry weight of the solids was calculated using the dry content, and the difference between wet and dry weight was used to determine how much water was already present in the material. Based on this value, the required amount of NaOH was dissolved in the correct amount of water to obtain the desired final NaOH concentration (see Appendix A.1 for

equations).

The wet solids and the prepared NaOH solution were placed into autoclaves, which were then transferred to a preheated polyethylene glycol bath. The soda pulping process was carried out at 170 °C for 2 hours and 25 minutes. After cooking, the autoclaves were placed in a cooling bath for about 5 minutes.

A Büchner funnel with a woven polypropylene mesh (31 μm) was placed on top of an Erlenmeyer flask. The pulp from the autoclaves was poured into the funnel and separated by filtration, with the flask connected to a vacuum line to speed up the process. The autoclaves were then rinsed with water, and the rinsing water was added to the funnel to recover any remaining solid material.

The recovered solid material was then defibrillated using a pulp disintegrator. For defibrillation, one batch of pulp was mixed with 1 L of deionized water and processed for 12 minutes. The resulting slurry was filtered again using the same setup and washed until the filtrate reached neutral pH as determined using pH strips. The pulp was then allowed to dry at room temperature.

3.4 Dry content

A small piece of the material was weighed in a plastic bottle and placed in a drying oven at 105 °C overnight in a Termaks drying oven. After drying, the sample was weighed again. The dry content was calculated as the ratio of the oven-dried weight to the initial wet weight.

3.5 Cold caustic extraction

The extraction procedure was based on the method reported by Sun, Lawther and Banks [41]. 1 wt% pulp was dispersed in 1.5 wt% NaOH and stirred at room temperature (20 °C) for 2 hours. The mixture was then filtered through a 31 μm mesh and washed with 2 L of water until the pH was neutral.

3.6 Dissolution

3.6.1 Aqueous NaOH–ZnO

Before dissolution, the fibers were shredded to about 0.5 mm using a Retsch mill. A so-called freeze-thawing method was used similar to the one reported by Budtova and Navard, using 2.5 wt% cellulose dissolved in 8% NaOH and 1% ZnO solution [42]. ZnO was first mixed with NaOH and a small amount of water until the solution appeared clear. The cellulose was then mixed with water and the NaOH/ZnO solution for approximately 1–2 minutes before being stored in a freezer at -20 °C overnight. The samples were then allowed to thaw while stirring before being analyzed using optical microscopy. For samples showing poor dissolution, a vortex mixer was applied prior to microscopy analysis, as mechanical agitation was expected to disentangle undissolved fiber aggregates

and improve homogeneity.

3.6.2 EMIMAc

Dissolution tests were also performed using 1-ethyl-3-methylimidazolium acetate (EMIMAc). A total of 2 g EMIMAc was used as solvent, with a cellulose concentration of 2 wt% corresponding to 0.04 g dry cellulose. Assuming a dry matter content of 80%, approximately 0.05 g of pulp was weighed out to obtain the target amount of dry cellulose. Dissolution was carried out at 80°C for 1 hour.

3.7 Analysis

3.7.1 Intrinsic viscosity (IV)

The limiting viscosity number of the pulp was measured using an ISO standard method 5351 with a dilute cupri-ethylenediamine (CED) solution.

Approximately 250 mg of each sample was weighed into a polyethylene dissolving bottle with a screw cap. A separate portion was weighed for dry matter content determination. All measurements were carried out in duplicate. Care was taken to minimize exposure to air, as oxygen can degrade cellulose in CED solution.

Next, 25.0 ml of distilled or deionized water and three pieces of copper wire were added to the test portion. The bottle was closed and shaken until the sample was completely disintegrated.

Then, 25.0 ml of CED solution was added. Any remaining air was removed by gently squeezing the bottle. The sample had to dissolve completely with no lumps. Shaking was performed for about 30 seconds.

After dissolution, the bottle was placed in a constant-temperature bath until (25 ± 0.1) °C was reached and the solution was measured within 30 min.

Viscosity measurements were carried out using capillary-tube viscometers, each equipped with a water jacket and connected to a constant-temperature bath. The viscometers were rinsed with water before use. A sufficient volume of the prepared test solution was drawn into the viscometer by suction and allowed to flow freely. When the meniscus reached the upper mark, the timer was started, and the efflux time to reach the lower mark was measured to an accuracy of ± 0.2 s. At least two measurements were made for each sample. The repeatability of the measurements was assessed using a $\pm 0.5\%$ agreement criterion. The mean value was then calculated.

Attempts were also made to measure IV of pretreated samples before soda pulping. However, the pulp did not fully dissolve in CED solution even after grinding, and in some cases undissolved particles blocked the capillary during measurement. IV measurements were therefore only carried out on pulp samples after soda pulping.

3.7.2 Compositional analysis

Two sample sizes were used depending on the analysis method: approximately 200 mg of sample (dry weight) for standard analysis, and approximately 30 mg of sample (dry weight) for microanalysis. The ground samples were dried overnight at 105 °C, then removed and placed in a desiccator to cool before weighing. Three milliliters of 72% H₂SO₄ were added and stirred carefully with a glass rod. For microanalysis, 0.45 ml of 72% H₂SO₄ was added. The samples were impregnated by placing them in a desiccator connected to a vacuum water aspirator for 15 minutes. The beakers were then placed in a 30 °C water bath for 60 minutes. The samples were stirred twice during this period.

The samples were then diluted with 84 g of deionized water. For microanalysis, 12.6 g of deionized water was used. The beakers were autoclaved at 125 °C for 60 minutes.

Each sample was removed from the autoclave and immediately filtered. The beakers and glass rods were rinsed with a small amount of warm deionized water, and the rinses were also filtered using a funnel and suction flask connected to a water aspirator. The hydrolysate (filtrate) was collected in a 100 ml volumetric flask; for microanalysis, a 25 ml volumetric flask was used instead. The suction flask was subsequently rinsed with hot deionized water to ensure complete recovery of the material.

The glass filters were removed, cooled in a desiccator, and dried overnight at 105 °C for determination of Klason lignin. After drying, the filters were weighed and the masses recorded for subsequent calculation of Klason lignin, defined as the acid-insoluble lignin fraction remaining after complete sulfuric acid hydrolysis and expressed as a percentage of the dry sample weight. For the 0.2% H₂SO₄ samples at EA 0.48 and EA 0.96, initial measurements gave inconsistent results, likely due to incomplete degradation of the pulp during acid hydrolysis. These samples were therefore ground to a smaller particle size and the measurements were repeated.

The hydrolysates were diluted before analysis of the carbohydrates in solution:

- 10× dilution: 2 ml of fucose solution and 5 ml of hydrolysate, diluted to 50 ml in a volumetric flask.
- 50× dilution: 2 ml of fucose solution and 1 ml of hydrolysate, diluted to 50 ml in a volumetric flask.

The solutions were syringe-filtered into labeled High-Performance Liquid Chromatography (HPLC) vials. The filter was pre-wetted by injecting the first portion into waste.

For acid-soluble lignin (ASL) analysis using UV measurement, the 10× dilution was used. If the absorbance exceeded 1, the 50× dilution was used instead. Absorbance was measured at 205 nm using a UV-Vis spectrophotometer (Specord 205, Analytik Jena).

3.7.3 Microscopy analysis

Optical microscopy was used to study how the pulp dissolves in cold alkali solvent and to investigate its potential suitability for textile fiber production. The analysis focused on morphological changes in the cellulose fibers, including swelling and ballooning effects, which indicates accessibility in the fibers.

The samples were observed using an optical microscope (Zeiss Axio Imager Z2, Carl Zeiss). Polarized light microscopy was performed at 10× magnification to evaluate the degree of cellulose fiber dissolution. Ten images were captured after thawing for each sample. Under polarized light with constant light intensity, intact undissolved fibers appear bright due to their crystalline birefringent structure, while dissolved fibers appear dark. Image analysis was performed using Fiji (ImageJ). Each image was converted to 8-bit grayscale, and a fixed intensity threshold of 20–255 was applied to distinguish undissolved fibers from the background. A minimum particle size of 10 pixels was set to exclude noise. The Analyze Particles function was then used to measure the total area of bright regions, corresponding to undissolved fibers, in each image. The remaining undissolved fiber area after dissolution was quantified as an indicator of dissolution quality [43].

3.7.4 Water retention value

Approximately 0.3 g of dried fibers were used. The pulp was placed in approximately 6 ml of deionized water and shaken to ensure fiber separation and left for 1 h prior to water retention value (WRV) measurement. Dry containers were pre-weighed before use. The samples were centrifuged in tubes with a diameter of 13 mm using a polyamide mesh filter (31 μm) at a centrifugal force of 3000 RCF for 30 minutes.

The centrifuged pulp was transferred to the pre-weighed dry container, which was then weighed together with the wet pulp. The samples were dried for 4 h at 105 °C. After drying, the containers were weighed with the dry fibers. The WRV was then calculated according to Equation 3.1, where m_1 is the mass of the centrifuged wet fibers and m_2 is the dry mass of the fibers:

$$\text{WRV} = \frac{m_1}{m_2} - 1 \quad (3.1)$$

3.7.5 Color measurement

The color of the pulp samples was measured using a Konica Minolta Chroma Meter CR-400 in conjunction with the SpectraMagic data software. Each sample was photographed three times at three different angles, giving nine images per sample in total. The measurements provided L , $a(\text{D65})$, and $b(\text{D65})$ values, corresponding to the CIE $L^*a^*b^*$ color space. L^* represents lightness (0 = black, 100 = white), a^* represents the green–red axis, and b^* represents the blue–yellow axis.

The color difference between each sample and a reference material was calculated using the following equation, based on the three-dimensional Euclidean distance:

$$\Delta E = \sqrt{(L_1^* - L_2^*)^2 + (a_1^* - a_2^*)^2 + (b_1^* - b_2^*)^2} \quad (3.2)$$

where L_1^* , a_1^* , and b_1^* correspond to the sample, and L_2^* , a_2^* , and b_2^* correspond to the reference material. The reference material was a dissolved cellulose mass. A smaller ΔE value indicates greater similarity in color to the reference, while a larger value indicates a greater color difference.

4. Results and Discussion

This chapter presents the results of the pretreatment and soda pulping experiments, followed by an analysis of the pulp properties and their suitability for textile fiber production. Wheat straw was used as the primary feedstock, with grass included as a secondary feedstock to investigate whether the process can be applied to other annual plants.

The pretreatment conditions varied in solvent type, including hot water and ethanol/water mixtures at 50% and 65% ethanol concentration, as well as sulfuric acid concentration and hydrochloric acid. The effective alkali (EA), shown in Table 4.3 and Table 4.4, was calculated based on both the NaOH concentration and the liquid-to-solid (L/S) ratio, since a higher L/S ratio increases the total amount of NaOH per gram of dry material. The L/S ratio was initially set to 8.3 (EA 0.332) but was later adjusted to 12 (EA 0.480–0.960) to increase the effective alkali. In the first experiments, the absorbed water in the pretreated straw was not fully considered when calculating the NaOH concentration, resulting in a real concentration of approximately 3.5% instead of 4%. Both the L/S ratio and NaOH concentration were therefore recalculated based on dry mass in all following experiments to ensure consistent conditions.

The pretreatment mass yields ranged from 50 to 81%, and the total process yields from 17 to 40%, as shown in Tables 4.1, 4.2, 4.3 and 4.4. The 50% ethanol pretreatment was performed twice to assess process variability, resulting in mass yields of 60% and 70%, respectively, the difference in mass yield indicates some variation in the pretreatment process, likely due to natural variation in the raw material.

Table 4.1: Pretreatment conditions and mass yield for wheat straw samples. All samples were treated at 175 °C for 2 h with a liquid-to-solid ratio of 12.

Sample	Solvent	H ₂ SO ₄ (%)	HCl (%)	Mass yield (%)
Hot water	100% Water	–	–	62
Hot water / 0.10% HCl	100% Water	–	0.10	51
50% EtOH	50% Ethanol	–	–	60
50% EtOH	50% Ethanol	–	–	70
65% EtOH	65% Ethanol	–	–	81
50% EtOH / 0.10% acid	50% Ethanol	0.10	–	78
50% EtOH / 0.15% acid	50% Ethanol	0.15	–	70
50% EtOH / 0.20% acid	50% Ethanol	0.20	–	50

Table 4.2: Pretreatment conditions and mass yield for the grass sample. The sample was treated at 175 °C for 2 h with a liquid-to-solid ratio of 12.

Sample	Solvent	H ₂ SO ₄ (%)	Mass yield (%)
50% EtOH (Grass)	50% ethanol	–	62

Table 4.3: Soda pulping conditions and mass yield for wheat straw samples. All samples were treated at 170 °C for 2 h and 25 min. EA refers to the effective alkali, expressed as g NaOH/100 g dry raw material.

Sample	L/S	NaOH (%)	EA	Dry content (%)	Pulping yield (%)	Total yield (%)
50% EtOH	8.3	3.5	0.332	12	68	40
50% EtOH / 0.15% acid	8.3	4	0.332	19	47	33
Hot water / 0.10 % HCl	14	4	0.56	-	–	31
Hot water	8.3	4	0.332	–	50	30
50% EtOH / 0.2% acid	12	4	0.48	20	51	26
50% EtOH / 0.2% acid	12	8	0.96	20	33	17
50% EtOH	12	4	0.48	14	41	29
50% EtOH	12	8	0.96	14	37	26
65% EtOH	12	4	0.48	13	37	30
65% EtOH	12	6	0.72	13	32	26
50% EtOH / 0.10% acid	12	4	0.48	13	42	33
50% EtOH / 0.10% acid	12	6	0.72	13	29	23

Table 4.4: Soda pulping conditions and mass yield for the grass sample. The sample was treated at 170 °C for 2 h and 25 min. EA refers to the effective alkali, expressed as g NaOH/100 g dry raw material.

Sample	L/S	NaOH (%)	EA	Dry content (%)	Pulping yield (%)	Total yield (%)
GH	12	4	0.48	13	38	24

4.1 Pulp composition

4.1.1 Effect of pretreatment solvent

The effect of pretreatment solvent on pulp composition and color was investigated by comparing 50% ethanol/water and 65% ethanol/water pretreatments under conditions without acid with different effective alkali. Glucose content reflected the cellulose fraction of the pulp, while non-glucose sugars such as arabinose, rhamnose, galactose, xylose, and mannose represented remaining hemicelluloses. For dissolving-grade pulp suitable for textile production, high glucose purity, low hemicelluloses, and low lignin were all important, since remaining lignin reduces fiber flexibility and quality.

The composition (wt%) of final pulps and the total mass yield is shown in Figure 4.1. The 65% ethanol condition at EA 0.72 showed the highest glucose content (wt%) combined with both low Klason lignin and low hemicelluloses content, suggesting this condition gave the highest cellulose purity. This agreed with Åkesson and Skotte, who found that higher ethanol concentrations improve lignin removal. Higher alkali charge (EA 0.96) in the 50% ethanol series reduced hemicelluloses content, however this sample also retained

relatively high Klason lignin, and the low total mass yield should be considered when interpreting the wt% composition. The 50% ethanol condition gave the highest total recovered material overall, indicating a trade-off between yield and purity [44].

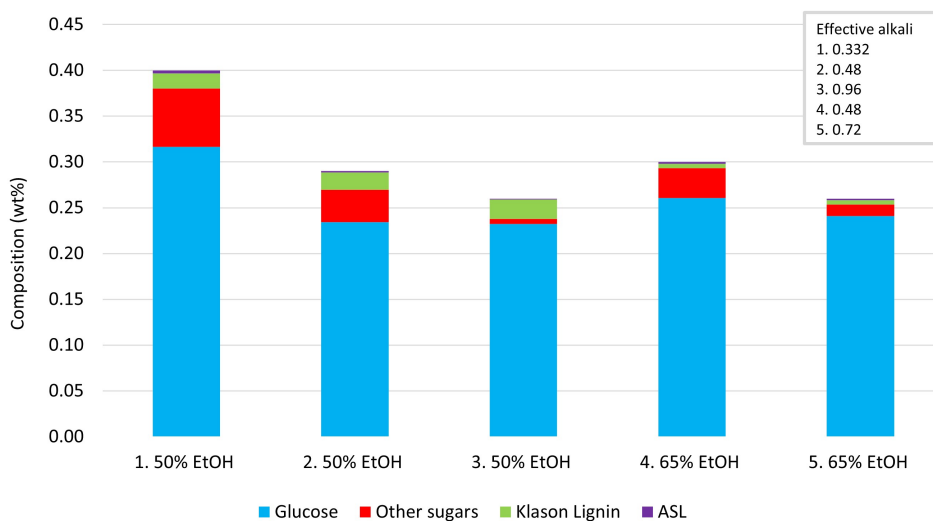


Figure 4.1: Composition of total mass yield (wt%) after pretreatment with different concentration of ethanol/water.

When considering component yields relative to the initial biomass (Figure 4.2), the 65% ethanol condition at EA 0.48 showed among the highest glucose yield alongside the lowest Klason lignin yield, indicating efficient delignification while keeping cellulose losses low. However, its hemicelluloses yield was slightly higher compared to both 65% ethanol at EA 0.72 and 50% ethanol at EA 0.96. Together, these results suggested that 65% ethanol conditions offered the most favorable balance between delignification and glucose yield, with EA 0.72 giving higher pulp purity and EA 0.48 giving higher glucose yield relative to the initial biomass. The complete composition data are presented in Appendix A.2.

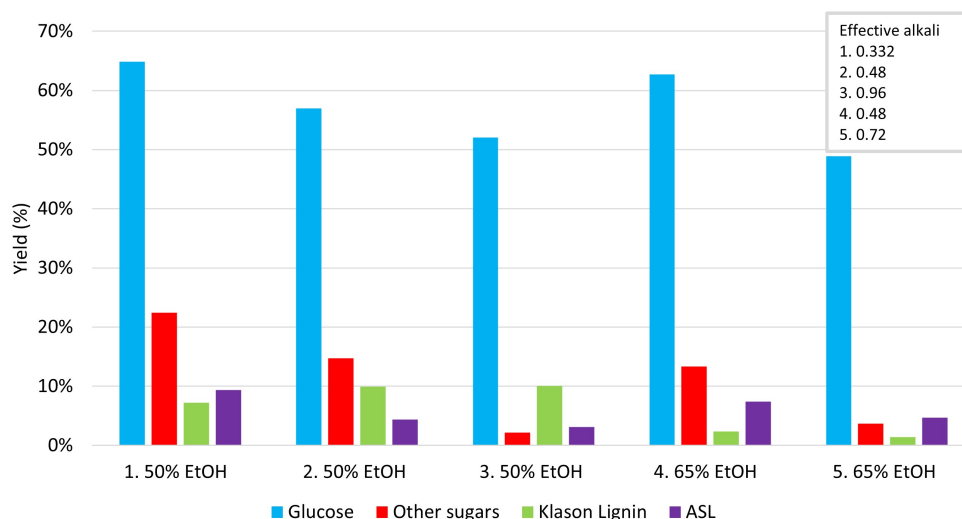


Figure 4.2: Component yields from wheat straw (wt%) after pretreatment with different concentration of ethanol/water, expressed relative to initial biomass.

The color difference (ΔE) between the pulp samples and the reference, a dissolving pulp

provided by TreeToTextile, is shown in Figure 4.3. A lower ΔE indicated that the sample was closer in color to the reference. Increasing ethanol concentration led to a larger color difference, meaning the pulp color moved further away from the reference. However, the L-values, which represent brightness, showed no major variation between the pretreatment or pulping conditions (Appendix A.3), indicating that the whiteness of the pulp was not strongly affected by solvent choice. This difference was therefore mainly related to color tone rather than whiteness. The distribution of the cellulose samples in the A and B color space is presented in Appendix A.3.

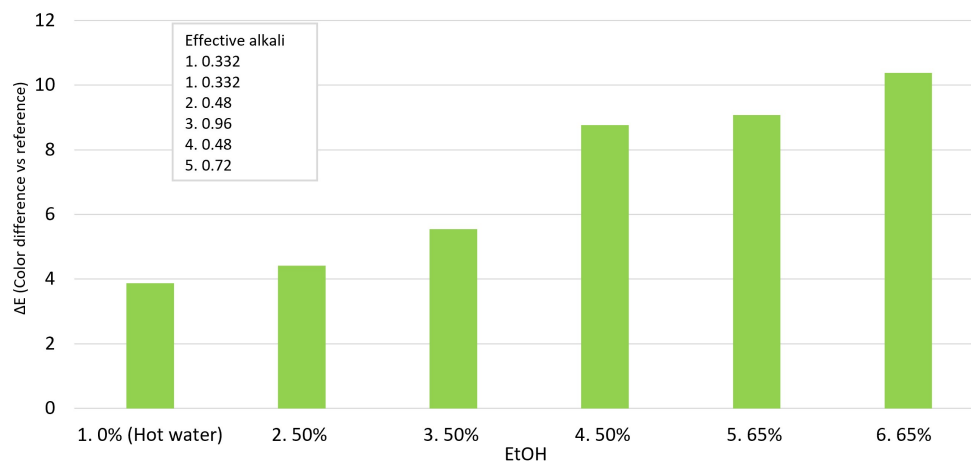


Figure 4.3: color difference (ΔE) between cellulose pulps and reference

4.1.2 Effect of acid concentration

This section examines how acid concentration affected pulp composition and color, with the pretreatment solvent kept constant at 50% ethanol/water. In the HCl treatment, hot water was used as the pretreatment solvent. Images of the pulp at different stages of the process are shown in Figure 4.4. Without acid, the wheat straw retained its original structure after pretreatment. In contrast, with acid treatment, the structure began to break down before pulping, indicating that the acid had an effect on the pulp structure at this stage. After soda pulping, however, both samples showed a similar fibrous texture.



Figure 4.4: Top row: pretreatment of cellulose without acid (left) and soda pulping (right). Bottom row: pretreatment with acid (left) and soda pulping (right)

As in the previous section, glucose content reflected the cellulose fraction, while non-glucose sugars indicated remaining hemicelluloses. High glucose purity, low hemicelluloses, and low lignin were all desirable for dissolving-grade pulp suitable for textile production.

The effect of acid concentration on composition was less clear than the effect of ethanol concentration seen in the previous section. Among the conditions tested, 0.1% H_2SO_4 at EA 0.48 gave the highest glucose content and highest recovered material, though it did not give the lowest hemicelluloses content. The 0.1% H_2SO_4 condition at EA 0.72 showed a good balance, with low hemicelluloses, low Klason lignin, and low ASL, while still maintaining a reasonably high glucose content. At higher acid concentrations and higher EA, the total recovered material decreased, with 0.2% H_2SO_4 at EA 0.96 giving the lowest yield. This indicated that combining high acid concentration with high effective alkali led to the greatest degradation of the material (Figure 4.5).

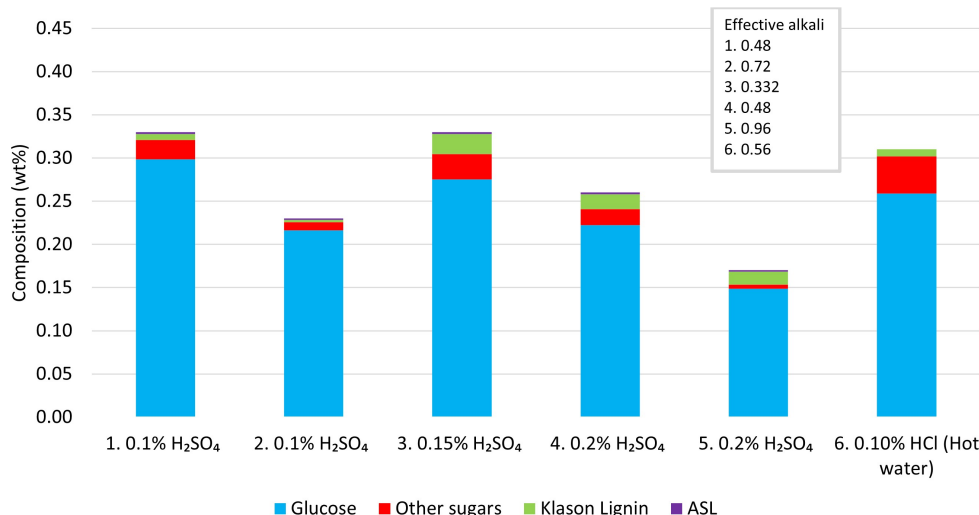


Figure 4.5: Composition of recovered solids (wt%) after pretreatment with varying H₂SO₄ concentrations in 50% ethanol/water and one sample with hot water and HCl.

When comparing component yields as a percentage of the untreated wheat straw (Figure 4.6), 0.1% H₂SO₄ at EA 0.48 and 0.10% HCl at EA 0.56 gave the highest glucose yield. 0.1% H₂SO₄ at EA 0.72 showed the lowest impurity content, although lower values might have been expected for 0.2% H₂SO₄ at EA 0.96. This suggested that both acid concentration and NaOH concentration improved treatment efficiency, however the effect seems to level off at higher concentrations.

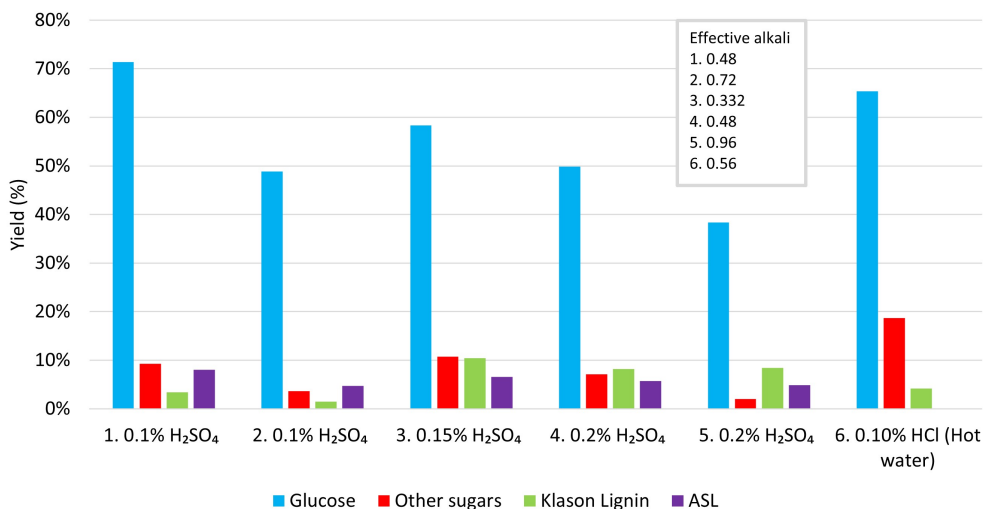


Figure 4.6: Component yields from wheat straw (wt%) with varying H₂SO₄ concentration in 50% ethanol/water pretreatment and one sample with hot water and HCl.

The color difference (ΔE) relative to the reference dissolving pulp is shown in Figure 4.7. In contrast to the ethanol results, increasing H₂SO₄ concentration led to a smaller (ΔE) meaning the pulp color moved closer to the reference. The HCl sample gave a similar (ΔE) to the 0.15% H₂SO₄ condition, suggesting a comparable effect on pulp color despite the different acid type and solvent used. As in the previous section, the L-values showed little variation (Appendix A.3), indicating that the differences were mainly in color tone

rather than whiteness. The distribution of the cellulose samples in the A and B color space is presented in Appendix A.3.

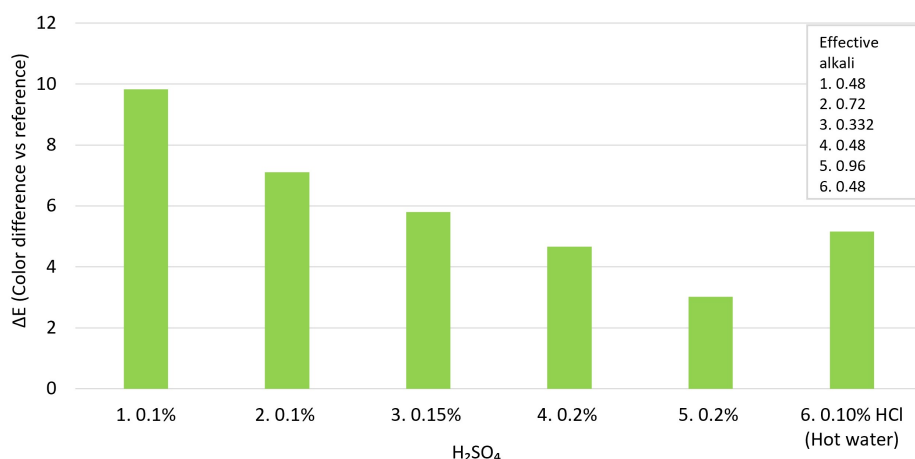


Figure 4.7: Color difference (ΔE) between cellulose pulps and reference

4.1.3 Effect of extraction

The extraction step was performed using 1.5 wt% NaOH at room temperature in order to remove remaining hemicelluloses after soda pulping. The composition values shown in Figure 4.8 are based on the total wt% and were not recalculated according to the recovered mass after extraction. In general, the extraction step slightly increased the glucose purity while reducing the amount of other sugars, indicating that hemicelluloses were not completely removed. However, the reduction in Klason lignin was clearer for the samples treated at EA 0.96, although the effect was still relatively small. For the sample treated at EA 0.48, the extraction reduced the hemicelluloses content to some extent, but the improvement in pulp purity was less clear.

It should be noted that the first Klason lignin measurements for some extracted samples gave inconsistent values. This was likely because the samples had not been fully degraded during the Klason lignin analysis. To improve the measurements, the samples were ground to a smaller particle size and the analysis was repeated, resulting in more reliable values.

The full compositional data of all samples are presented in Appendix A.2.

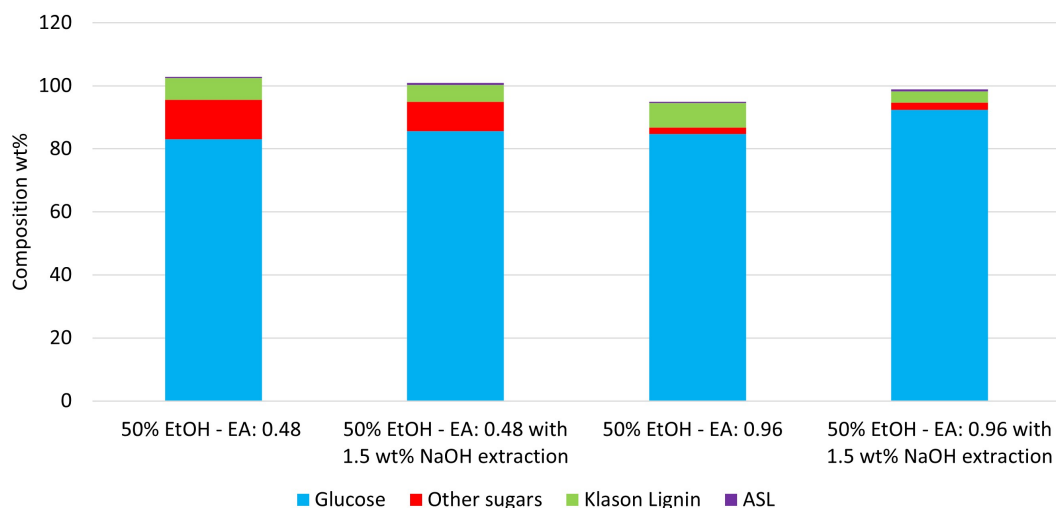


Figure 4.8: Effect of 1.5 wt% NaOH extraction on composition in total wt%. The values were not recalculated based on the recovered mass after extraction.

The color difference (ΔE) between the cellulose pulps and the reference dissolving pulp provided by TreeToTextile is shown in Figure 4.9. A lower ΔE value means that the sample color is closer to the reference. No clear correlation was observed between extraction and color difference, since the values before and after extraction were relatively similar for both conditions.

No significant changes were observed in either the L-value or the color difference ΔE after extraction. The L-values showed only minor variation between the samples (Appendix A.3), indicating that the whiteness of the pulp was largely unaffected by the extraction step. The differences observed were instead mainly related to color tone, as shown in Figure 4.9. The distribution of the cellulose samples in the A and B color space is presented in Appendix A.3.

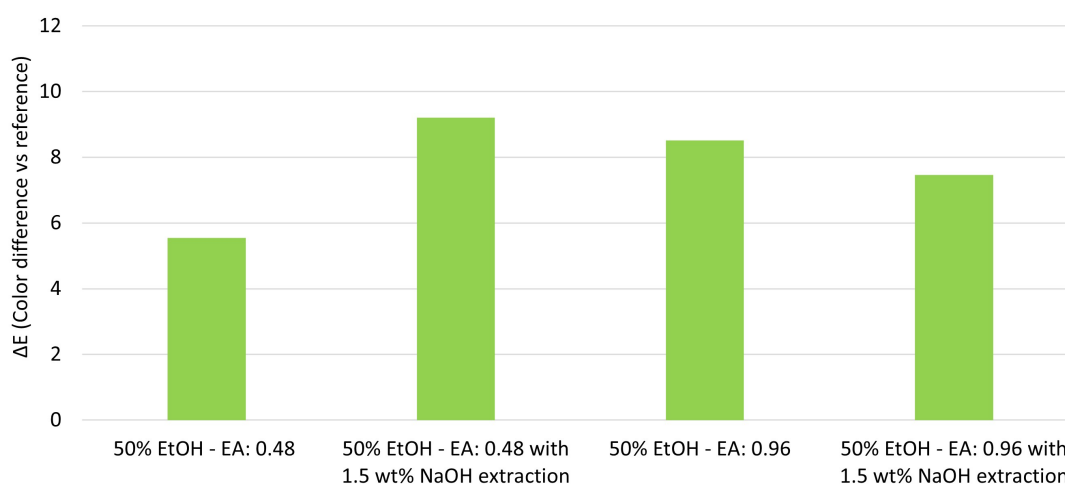


Figure 4.9: Color difference (ΔE) between cellulose pulps and reference

4.1.4 Feedstock comparison

The grass sample was treated under the same conditions as the selected wheat straw reference condition (50% ethanol pretreatment and EA 0.48 during soda pulping). The purpose of this experiment was to investigate whether the process developed for wheat straw could also be applied to another annual plant feedstock. Previous studies have shown that grass cellulose can be more sensitive during processing and may give lower intrinsic viscosity than wheat straw under similar conditions [45].

The composition of the grass sample is shown in Figure 4.10. The results showed that the grass sample contained a relatively high glucose content together with low amounts of hemicelluloses, Klason lignin and ASL. Compared to the wheat straw sample treated under the same conditions, the grass sample showed a similar glucose content (wt%) but lower hemicelluloses and notably lower Klason lignin content, suggesting that the pretreatment and soda pulping conditions were particularly effective for delignification of grass.

Although some impurities remained in the grass sample, the overall composition indicated that strong acid treatment was not necessary for this feedstock. The relatively low amounts of lignin and hemicelluloses indicated that the material could be processed under moderate conditions while still producing a cellulose-rich pulp. However, the glucose content of the grass sample was slightly lower than the other wheat straw samples, which may have suggested that grass cellulose was more sensitive to degradation during treatment. This agreed with previous studies reporting that grass fibers are more sensitive than wheat straw during pulping and pretreatment processes [45].

The full compositional data of all samples are presented in AppendixA.2.

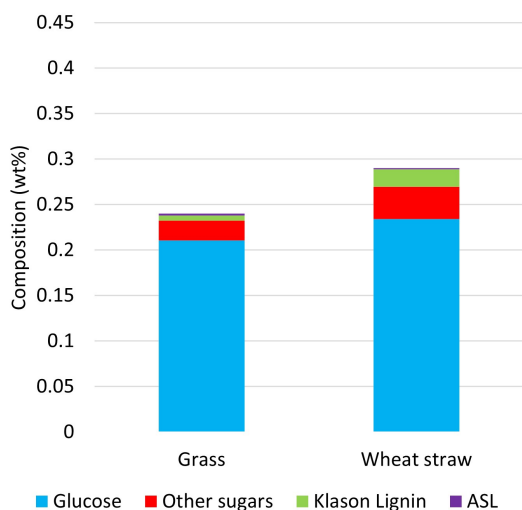


Figure 4.10: Composition of recovered material (wt%) for the grass sample and the wheat straw sample treated under the same conditions (50% ethanol, EA 0.48).

The color difference (ΔE) between the grass pulp and the reference dissolution mass provided by TreeToTextile is shown in Figure 4.11. A lower ΔE value means that the sample color is closer to the reference. The grass sample showed a larger ΔE value than

the wheat straw samples, indicating a greater color difference from the reference material. None of the wheat straw samples reached as high a ΔE value as the grass sample, indicating that the grass pulp had a darker or different color tone.

The L-values showed no major variation between the samples (Appendix A.3), indicating that the brightness was relatively similar for both grass and wheat straw pulps. The differences were instead mainly related to color tone, which was reflected in the a and b color values presented in Appendix A.3. This suggested that the larger ΔE value of the grass sample was not primarily caused by lower brightness, but rather by differences in color. Since the grass sample also showed relatively low lignin content, the color difference could not be explained only by residual lignin.

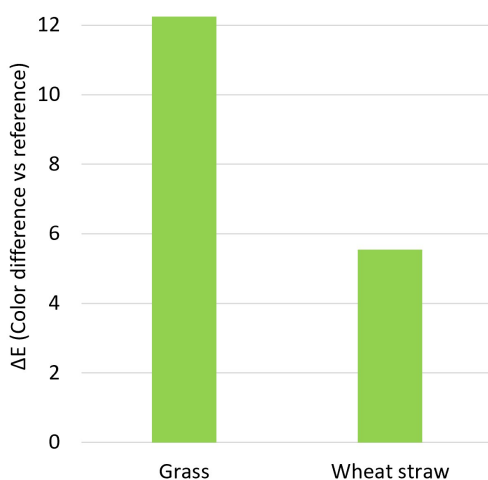


Figure 4.11: Color difference (ΔE) between cellulose pulp and reference for the grass sample and the wheat straw sample treated under the same conditions (50% ethanol, EA 0.48).

Overall, the results showed that the process developed for wheat straw could also be applied to grass, since the grass sample achieved low lignin and hemicelluloses contents together with a relatively high cellulose content. However, the lower glucose yield and larger color difference indicated that some process adjustments may be necessary to further optimise the treatment conditions for grass-based feedstocks.

4.2 Pulp properties

4.2.1 Degree of polymerisation

Intrinsic viscosity (IV) is an important parameter for dissolving-grade pulp, as it reflects the average molecular weight and degree of polymerisation of cellulose chains. IV is reported in mL/g, which is the standard unit used in ISO 5351 and commonly applied in cellulose research. Although mL/g is not an SI unit, it is the accepted convention for this type of measurement.

The efflux times were measured in duplicate or triplicate, and the average values were used. Most samples showed good repeatability, while some showed larger variation between measurements. In some cases, the deviation exceeded the $\pm 0.5\%$ agreement criterion, particularly for samples with longer efflux times. This was likely due to higher sensitivity to small timing errors. However, the overall trends were considered reliable.

The measured intrinsic viscosities are presented in Table 4.5. In general, increasing effective alkali (EA) resulted in lower IV values, indicating increased cellulose depolymerisation during soda pulping. This was clearly seen for the 50% ethanol/water samples without acid, where IV decreased from 699 ± 1.93 at EA 0.332 to 494 ± 4.27 mL/g at EA 0.480 and further to 193 ± 0.80 mL/g at EA 0.960.

Within the same EA level, pretreatment conditions also influenced IV. At EA 0.480, the 65% ethanol sample showed lower IV than the corresponding 50% ethanol sample, suggesting increased cellulose degradation at higher ethanol concentration. The addition of acid further reduced IV values. For example, the 50% ethanol/water sample with 0.2% acid at EA 0.480 gave an IV of 332 ± 7.55 mL/g, compared with 494 ± 4.27 mL/g for the sample without acid. At higher acid concentration combined with high EA, IV values approached 200 mL/g, indicating strong cellulose degradation..

The liquid-to-solid (L/S) ratio also affected IV. Samples treated at $L/S = 12$ had higher effective alkali than those at $L/S = 8.3$, meaning more NaOH per gram of dry material. This likely contributed to greater cellulose degradation and lower IV values, showing that L/S ratio was an important process parameter in addition to solvent composition and acid concentration.

The grass sample showed lower IV than wheat straw under identical conditions. At 50% ethanol/water and EA 0.480, the grass sample gave an IV of 396 ± 1.38 mL/g, compared with 494 ± 4.27 mL/g for wheat straw. This supported previous findings that grass cellulose is more sensitive to chemical treatment than wheat straw [45].

An alkaline extraction step (1.5 wt% NaOH at room temperature) slightly increased IV at both EA levels, from 494 ± 4.27 to 533 ± 2.86 mL/g at EA 0.480 and from 193 ± 0.80 to 209 ± 1.97 mL/g at EA 0.960. This was likely due to the removal of low-molecular-weight hemicelluloses and remaining lignin, resulting in a higher average degree of polymerisation of the remaining cellulose fraction.

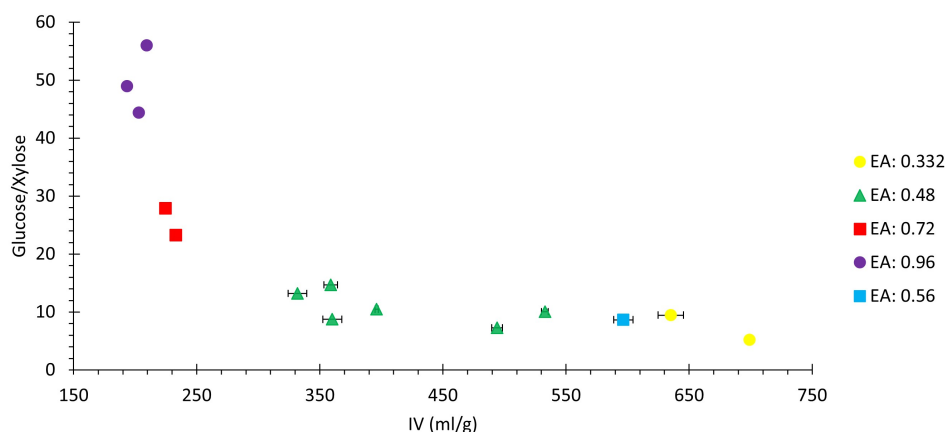
Table 4.5: Intrinsic viscosity (IV) for different cooking conditions grouped by treatment

Condition	EA	IV (ml/g) \pm SD
Ethanol/water without acid		
50% EtOH/water	0.332	699 \pm 1.93
50% EtOH/water	0.480	494 \pm 4.27
50% EtOH/water	0.960	193 \pm 0.80
65% EtOH/water	0.480	360 \pm 7.67
65% EtOH/water	0.720	233 \pm 4.48
50% EtOH/water (Grass)	0.480	396 \pm 1.38
Hot water	0.332	521
Ethanol/water with acid		
50% EtOH/water / 0.15% acid	0.332	635 \pm 10.38
50% EtOH/water / 0.2% acid	0.480	332 \pm 7.55
50% EtOH/water / 0.2% acid	0.960	203 \pm 1.48
50% EtOH/water / 0.1% acid	0.480	359 \pm 5.52
50% EtOH/water / 0.1% acid	0.720	225 \pm 1.90
Hot water / 0.10% HCl	0.480	597 \pm 7.88
Extraction		
50% EtOH/water - after extraction	0.480	533 \pm 2.86
50% EtOH/water - after extraction	0.960	209 \pm 1.97

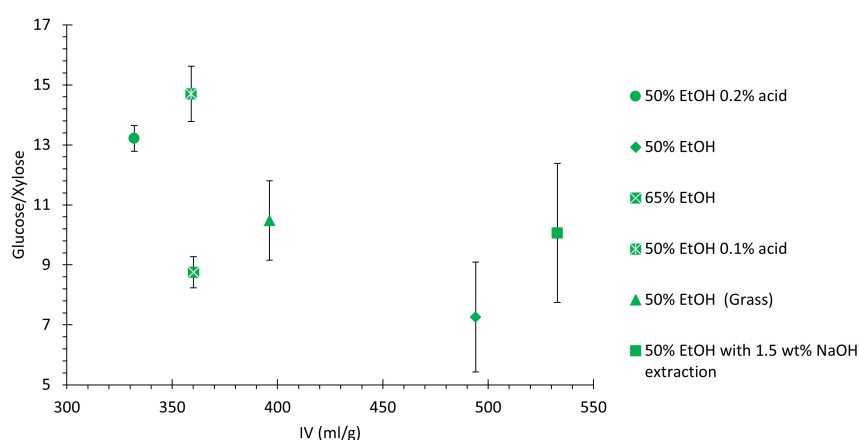
4.2.2 Cellulose purity and intrinsic Viscosity

A similar trend was observed between glucose/xylose ratio and intrinsic viscosity. Overall, higher glucose/xylose ratios tended to correspond to lower IV values, although the relationship was not strictly linear. At EA 0.96 and EA 0.72, relatively high purity was observed together with low IV values. However, at intermediate EA 0.48 the IV varied significantly between 350 and 750 mL/g, indicating that pretreatment conditions strongly influenced chain degradation.

When the analysis focused on an EA value of 0.48, the dominant influence of alkali concentration was reduced, which made it easier to compare the effects of solvent composition and acid addition more clearly. Under these conditions, lower IV values were observed for 50% ethanol with acid and 65% ethanol, indicating better control of cellulose degradation during processing. These results highlight a clear trade-off between purity and chain length: higher ethanol concentration or acid addition improved cellulose purity but was associated with increased chain degradation, suggesting that pretreatment conditions must be carefully balanced to achieve both high purity and sufficient molecular weight.



(a) All samples.



(b) EA = 0.48 only.

Figure 4.12: Relationship between cellulose purity (glucose/xylose ratio) and intrinsic viscosity (IV).

4.2.3 Mass yield and degree of polymerisation

At EA 0.48, both mass yield and IV varied strongly depending on pretreatment conditions, indicating that solvent and acid chemistry strongly influenced cellulose degradation at intermediate alkali levels, which are shown in Figure 4.13. To further investigate the EA 0.48 samples, the relationships between mass yield and WRV, and between mass yield and cellulose purity (glucose/xylose ratio), are shown in Figures 4.14 and 4.15, respectively. Among the EA 0.48 samples, IV was the dominant factor governing dissolution behaviour, as higher IV generally corresponded to a higher undissolved fraction.

However, when comparing samples with similar IV values, differences in dissolution behaviour were still observed. The 50% ethanol samples with acid addition (0.1% and 0.2% H_2SO_4) showed lower undissolved fractions compared to the 65% ethanol sample, despite having comparable IV values. These samples also showed higher cellulose purity (glucose/xylose ratio of 13.2-14.7 compared to 8.7) and lower WRV (1.2-1.5 compared to 2.0), suggesting that cellulose purity and fiber swelling capacity may also have influenced dissolution behaviour. However, as these properties varied simultaneously across

the samples, their individual contributions could not be fully distinguished based on the present data.

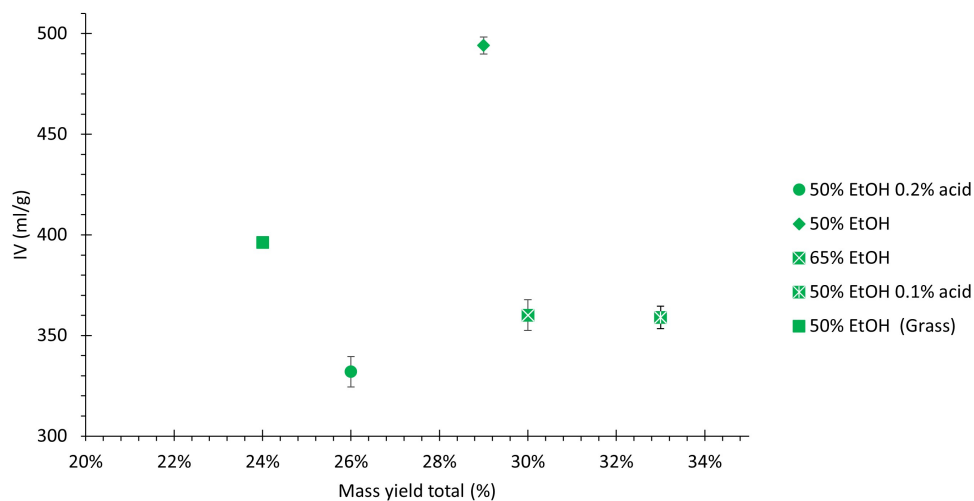


Figure 4.13: Relationship between mass yield (%) and intrinsic viscosity (IV) for EA 0.48 samples.

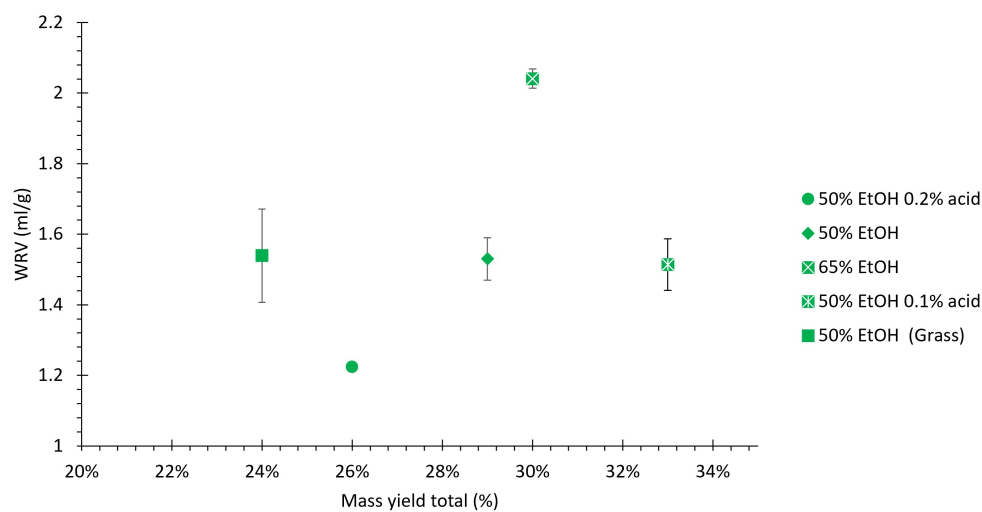


Figure 4.14: Relationship between mass yield (%) and WRV for EA 0.48 samples.

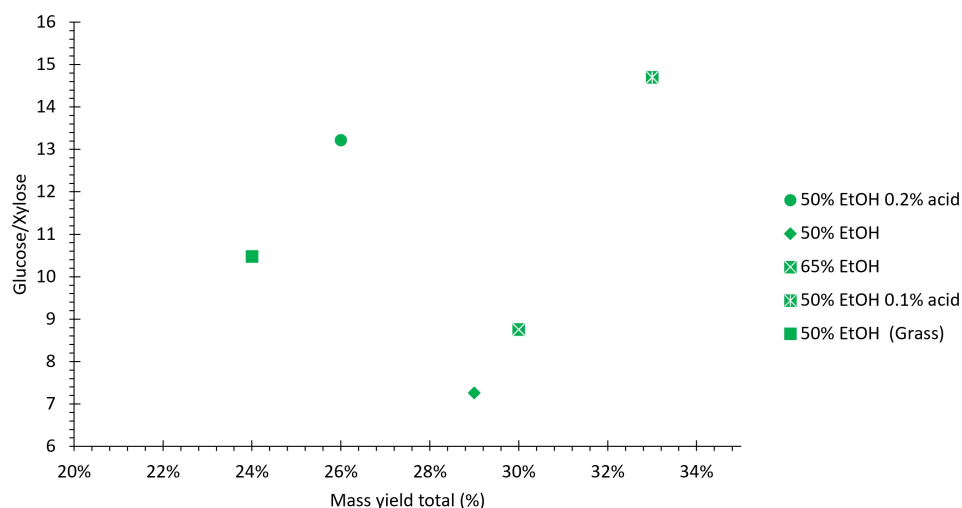


Figure 4.15: Relationship between mass yield (%) and cellulose purity (glucose/xylose ratio) for EA 0.48 samples.

4.2.4 Water retention value

Water retention value (WRV) is a measure of how much water a cellulose fiber can retain after centrifugation and is commonly used as an indicator of fiber swelling and accessibility. A high WRV means the fiber structure has many accessible pores and an open cell wall, while a low WRV indicates a more compact structure. This property is important for dissolving-grade pulp since sufficient swelling improves chemical accessibility during dissolution and fiber processing [39].

The WRV results for all samples are presented in Table 4.6.

Table 4.6: WRV values for different cooking conditions grouped by treatment.

Condition	EA	WRV \pm SD
Ethanol/water without acid		
50% EtOH/water	0.332	1.28 \pm 0.05
50% EtOH/water	0.480	1.53 \pm 0.06
50% EtOH/water	0.960	1.18 \pm 0.03
65% EtOH/water	0.480	2.04 \pm 0.03
65% EtOH/water	0.720	1.42 \pm 0.00
50% EtOH/water (Grass)	0.480	1.54 \pm 0.13
Ethanol/water with acid		
50% EtOH/water / 0.15% H ₂ SO ₄	0.332	1.45 \pm 0.04
50% EtOH/water / 0.2% H ₂ SO ₄	0.480	1.22 \pm 0.01
50% EtOH/water / 0.2% H ₂ SO ₄	0.960	1.18 \pm 0.03
50% EtOH/water / 0.1% H ₂ SO ₄	0.480	1.51 \pm 0.07
50% EtOH/water / 0.1% H ₂ SO ₄	0.720	1.39 \pm 0.02
Extraction		
50% EtOH/water (before extraction)	0.480	1.53 \pm 0.06
50% EtOH/water (after extraction)	0.480	1.37 \pm 0.03
50% EtOH/water (before extraction)	0.960	1.18 \pm 0.03
50% EtOH/water (after extraction)	0.960	1.07 \pm 0.05

The relationship between WRV and effective alkali is shown in Figure 4.16. For 50% ethanol/water without acid, WRV increased from 1.28 \pm 0.05 at EA 0.332 to 1.53 \pm 0.06 at EA 0.480, but then dropped to 1.18 \pm 0.03 at EA 0.960. This suggested that there was an optimal EA around 0.480, beyond which excessive alkali began to damage the fiber structure and reduce swelling capacity. This agreed with the IV results, where EA 0.960 also showed signs of excessive cellulose degradation.

The highest WRV was found for 65% ethanol/water at EA 0.480 (2.04 \pm 0.03), which was notably higher than the corresponding 50% ethanol condition (1.53 \pm 0.06). This indicated that higher ethanol concentration during pretreatment produced a more open and accessible fiber structure. Acid addition did not show a consistent effect on WRV; depending on the acid concentration and EA, WRV either increased slightly, decreased, or remained similar compared to samples without acid. This suggested that WRV was more strongly governed by the alkali treatment than by acid concentration during pretreatment. The grass sample showed a similar WRV value (1.54 \pm 0.13) compared to wheat straw (1.53 \pm 0.06) under the same conditions, indicating no significant difference.

Extraction reduced WRV in all cases, from 1.53 \pm 0.06 to 1.37 \pm 0.03 at EA 0.48 and from 1.18 \pm 0.03 to 1.07 \pm 0.05 at EA 0.96. This was likely due to the removal of accessible material from the fiber wall, such as hemicelluloses and lignin, which readily swelled and dissolved, thereby reducing the overall swelling capacity of the fiber. Despite the lower WRV, extraction improved cellulose purity, indicating a trade-off between fiber swelling and chemical purity.

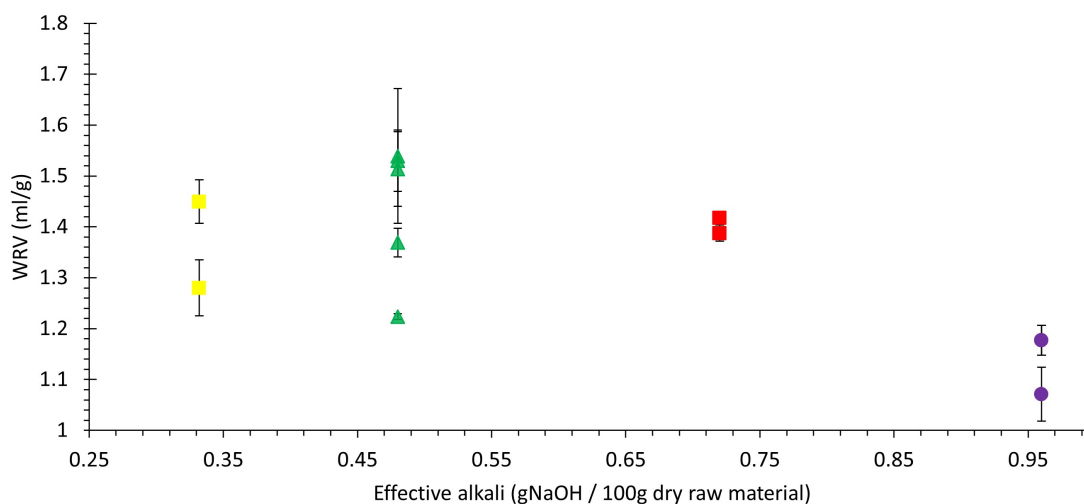
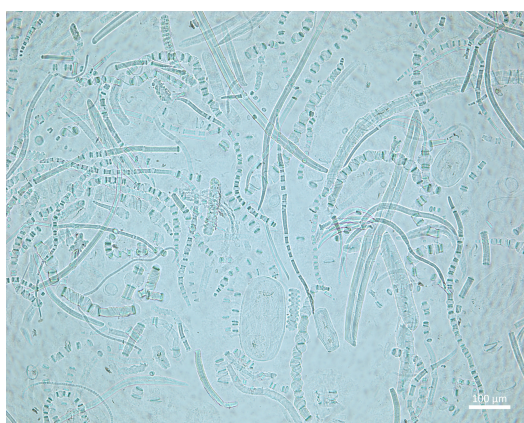


Figure 4.16: Relationship between water retention value (WRV) and effective alkali (EA) for all samples.

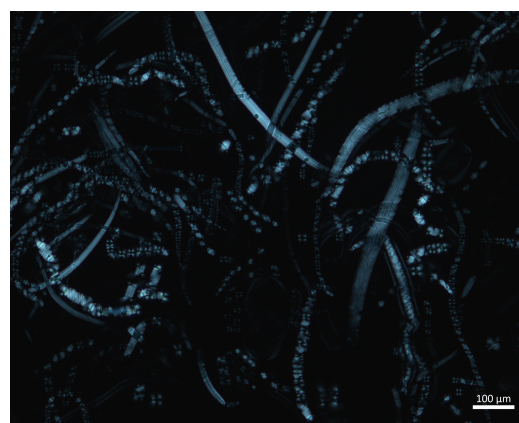
4.3 Dissolution

Cold alkali dissolution was used to evaluate the suitability of the pulp samples for textile fiber production. Due to high variability between images before freezing, only the images from the thawed stage were used for evaluation.

Bright-field microscopy was used to observe fiber morphology and swelling, while polarized light microscopy distinguishes undissolved crystalline regions (bright areas) from dissolved amorphous regions (dark areas). The figures below show the same sample and field of view imaged using bright-field and polarized light microscopy, respectively, with different optical settings (Figure 4.17).



(a) Bright field image.



(b) Polarized image.

Figure 4.17: Dissolution of 4% NaOH in 50% ethanol/water during thawing (12 L/S). Comparison between bright field and polarized light images.

The dissolution results showed large differences between samples, with some conditions giving nearly complete dissolution and others showing significant amounts of undissolved

fibers. Some samples showed poor reproducibility between repeated measurements, which could not be resolved by increasing dissolution volume or applying vortex blending. This indicated that the variability was related to inconsistent fiber aggregation and gelation within the sample, with uneven fiber distribution, rather than mixing alone.

A clear ballooning effect was observed during cold alkali dissolution, as shown in Figure 4.18. This behaviour indicated that the cellulose structure was opening up and becoming more accessible to the solvent. The ballooning phenomenon is an important indicator of fiber accessibility, as it reflects solvent penetration into the fiber wall. In the images, this appeared as enlarged swollen regions and partial fiber separation. In some cases, large bubble-like structures that were not fibers were also observed, which were seen in other samples as well. Overall, this suggested that the cellulose was reactive and capable of swelling.

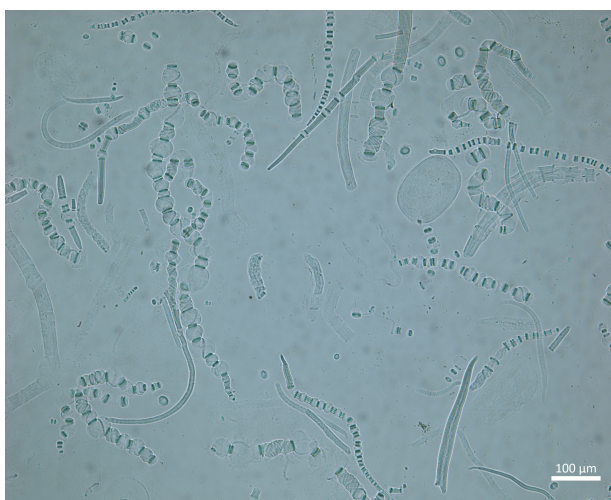
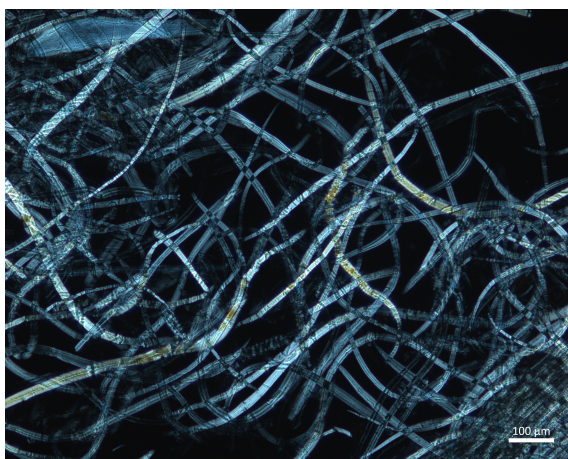


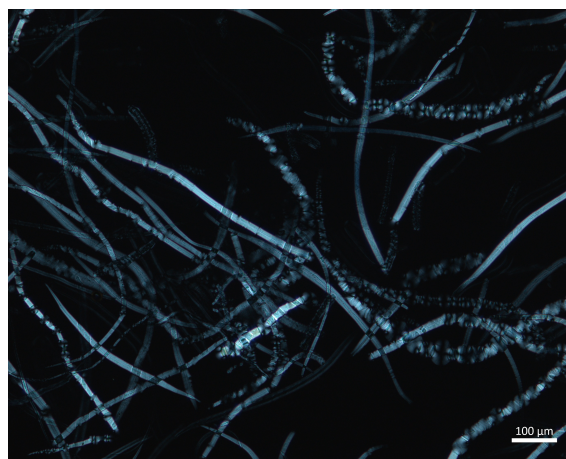
Figure 4.18: Bright-field microscopy image showing fiber swelling (“ballooning”) during dissolution of pretreated cellulose in 4% NaOH (50% ethanol/water, EA 0.480).

The sample that dissolved the least showed a large amount of undissolved fiber in the thawing image (Figure 4.19b). Ideally, no visible fibers should remain, since polarized light microscopy indicates crystalline regions that should disappear upon complete dissolution. The presence of strong bright regions in the polarized image confirmed incomplete dissolution and poor fiber accessibility.

The sample that dissolved the most showed only a small amount of remaining fiber in the thawing stage (Figure 4.20b). The polarized image contained fewer bright regions, indicating more complete dissolution and a higher fraction of dissolved cellulose. This indicated improved accessibility and fiber reactivity compared to the worst case.

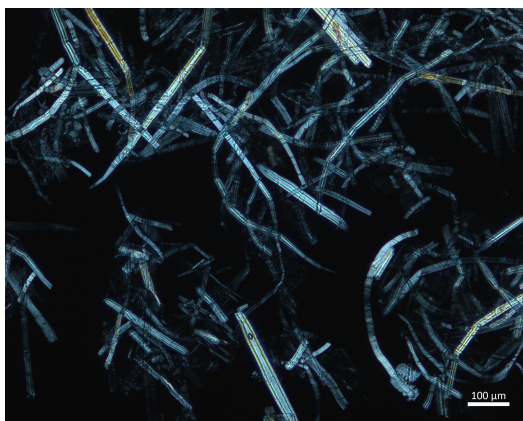


(a) Before thawing.

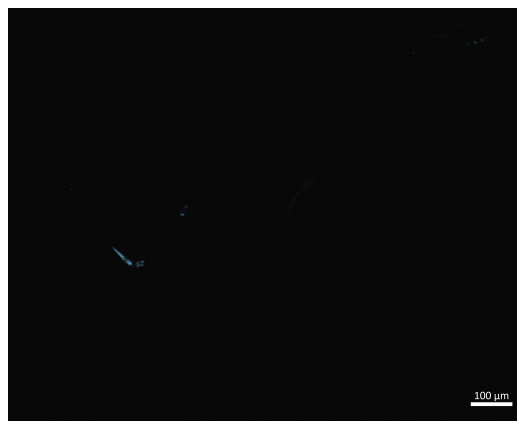


(b) During thawing.

Figure 4.19: Optical microscopy of the least effective dissolution condition (50% ethanol/water, EA 0.332). Polarized light images showing a high fraction of undissolved fiber.



(a) Before thawing.



(b) During thawing.

Figure 4.20: Optical microscopy of the most effective dissolution condition (50% ethanol/water, 0.2% H₂SO₄, EA 0.960). Polarized light images showing improved fiber dissolution and reduced crystalline regions.

An additional dissolution test using EMIMAc showed very little undissolved fiber across all samples, indicating that the cellulose could be dissolved under suitable solvent conditions. This indicated that the observed differences in the NaOH/ZnO system were likely related to the interaction between the solvent system and cellulose, rather than indicating that the cellulose was not dissolvable. The EMIMAc results are presented in Appendix A.4.

4.4 Connecting pulp properties and dissolution

This section compares all experimental results to identify the main factors that controlled dissolution behaviour and overall pulp quality. Instead of analysing each property

separately, the aim was to connect intrinsic viscosity, composition, mass yield, and dissolution performance to understand which parameters were most important for producing dissolving-grade pulp.

4.4.1 Dissolution and extraction

When comparing dissolution, defined as the undissolved area %, and extraction effects on IV (Figure 4.21), the results indicated that the 1.5 wt% NaOH extraction did not significantly change either the dissolution behaviour or the intrinsic viscosity (IV) of the samples.

The graph also showed the RSD values and the corresponding differences in the dissolution images. The RSD values at EA 0.480 were higher both before and after extraction, indicating more variable dissolution behaviour at this alkali level. In contrast, the EA 0.960 samples showed very low RSD values before and after extraction, suggesting more consistent and reproducible dissolution at higher alkali charge.

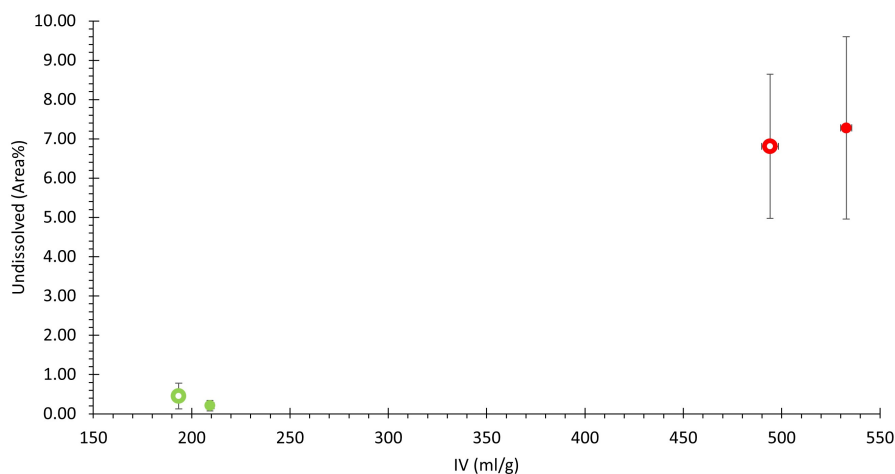


Figure 4.21: Relationship between intrinsic viscosity (IV) and undissolved in area% before and after 1.5 wt% NaOH extraction. Red points represent 50% ethanol samples at EA 0.48, green points represent EA 0.96. The white center indicate samples prior to extraction.

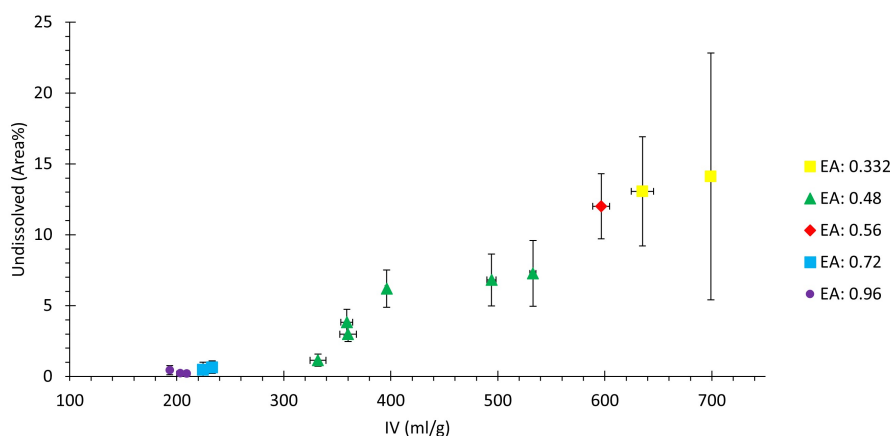
4.4.2 Dissolution and intrinsic viscosity

A clear trend was observed where lower IV generally corresponded to lower dissolution, while increasing EA led to improved dissolution. This indicated that both chain length and treatment conditions influenced fiber accessibility (Figure 4.22a).

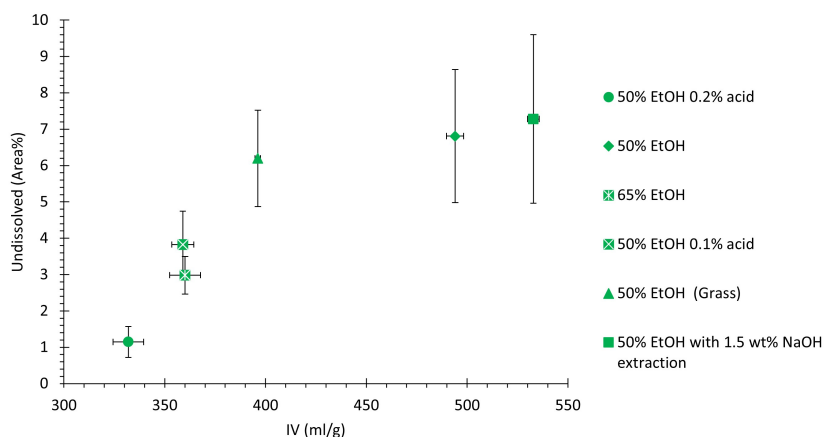
The EA 0.48 samples are shown in the second plot. It was observed that the highest IV and undissolved area were found for the 50% ethanol sample, both with and without extraction. The lowest IV and undissolved area were found for the 65% ethanol sample and the 50% ethanol sample with 0.1% acid, while the grass sample lay in the middle. The lowest values were observed for the 50% ethanol sample with 0.2% acid, indicating that higher acid concentration and ethanol content improved dissolution behaviour.

Overall, these results suggested that effective alkali was the dominant factor governing dissolution behaviour. At low EA, high IV and poor dissolution were observed, while increasing EA resulted in shorter cellulose chains and improved dissolution. However, at very high EA, excessive chain degradation was observed, which may negatively affect the properties of the resulting fiber.

The RSD values varied considerably between conditions, and a general trend was observed where higher IV corresponded to higher RSD values. Even though a vortex mixer was applied prior to microscopy analysis to those samples, it still showed large RSD values. This indicated that samples with longer cellulose chains and poorer dissolution also showed less consistent behaviour between repeat measurements. The EA 0.332 samples in particular showed notably higher RSD values compared to the other conditions.



(a) All effective alkali values.



(b) EA = 0.48 only.

Figure 4.22: Relationship between intrinsic viscosity (IV) and undissolved in area%.

4.4.3 Cellulose purity and dissolution

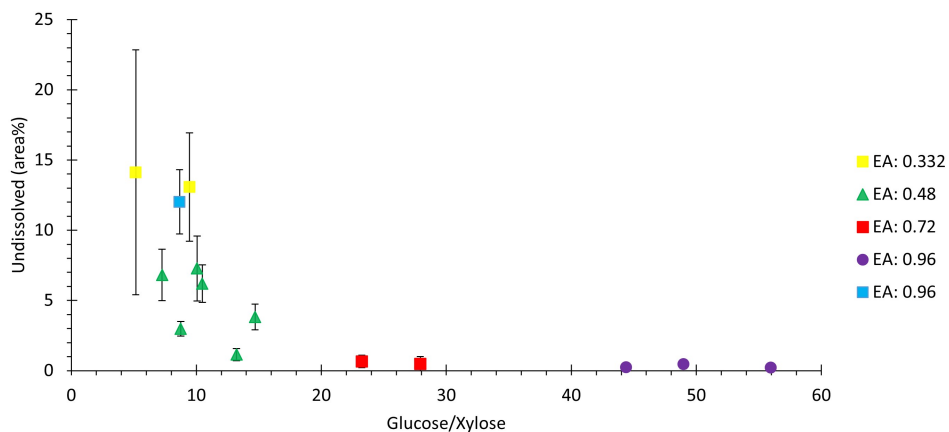
A more informative measure of pulp quality is the glucose/xylose ratio, since it reflects cellulose content relative to hemicelluloses. Glucose represent cellulose chains (the target product), while xylose and other non-glucose sugars originate from hemicelluloses. There-

fore, a high glucose/xylose ratio indicated high cellulose purity and low hemicelluloses content.

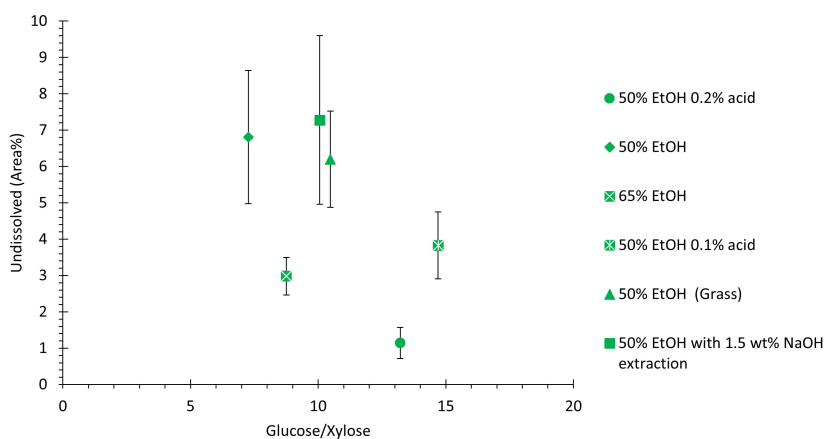
The results showed that samples with higher glucose/xylose ratios generally exhibited better dissolution. At EA 0.72 and EA 0.96, both high purity and good dissolution were observed. However, at EA 0.48 the results varied more strongly, indicating that other factors such as pretreatment conditions played a larger role in this region.

At EA 0.48, the results varied more strongly between samples, indicating that pretreatment conditions played a larger role at this alkali level. In general, the glucose/xylose ratios were similar, ranging from approximately 5 to 15. However, higher dissolution was observed for samples with higher ethanol and acid concentrations. Samples containing only 50% ethanol, as well as the grass sample, also showed higher RSD values.

Lower glucose/xylose ratios tended to also correspond to higher RSD values. Even though a vortex mixer was applied prior to microscopy analysis to those samples, it still showed large RSD values. This may have indicated that samples with higher cellulose purity but longer chain length dissolved less consistently under cold alkali conditions.



(a) All samples.



(b) EA = 0.48 only.

Figure 4.23: Relationship between cellulose purity (glucose/xylose ratio) and undissolved in area%.

4.5 Disclosure and declaration of AI use

AI-based tools were utilised to assist with data processing, code development and debugging, formatting of experimental results, content structuring, and language editing. All AI-generated contributions were reviewed and validated by the author.

5. Conclusion

Across all experimental conditions, effective alkali was the most important factor influencing both intrinsic viscosity and dissolution behaviour. Higher EA values consistently resulted in lower IV and improved dissolution, regardless of pretreatment solvent composition or acid concentration. However, a very high EA level (0.960) also caused a reduction in WRV, indicating that excessive alkali charge may begin to damage the fibre structure even though dissolution performance improves. Higher ethanol concentrations or the addition of acid promoted lignin removal, while the application of a moderate EA level of approximately 0.48–0.72 during soda pulping made it possible to achieve the target IV range while maintaining fibre integrity and avoiding a significant decrease in mass yield.

It should also be noted that pulp color appeared to be affected by the pretreatment conditions. Increasing the ethanol concentration produced a pulp color that differed more from the reference pulp, whereas acid addition resulted in a pulp color more similar to the reference material. This indicates a trade-off between pretreatment efficiency and pulp appearance, which is important to consider for the following processing stages, particularly if bleaching is required.

The extraction method used in this study reduced the hemicelluloses content to some extent and slightly increased IV, but did not significantly improve cellulose dissolution. However, since only two samples were evaluated, it is difficult to draw conclusions. Further investigation of alternative extraction conditions or methods could therefore be of interest in future work.

The grass sample showed a somewhat different response to the processing conditions compared to wheat straw, suggesting that annual plants of different origins may require process adjustments to achieve optimal results. The grass material appeared to be more sensitive to the treatment conditions; however, from an environmental perspective, this sensitivity may also be advantageous, as it could allow the use of less concentrated chemicals during processing. Overall, the results demonstrated that a mild process could be designed to produce a cellulose-rich pulp suitable for dissolving applications from annual plant feedstocks, which is encouraging in comparison to wood-based processes that typically require more intensive treatment conditions.

6. Future work

Future work could focus on using different parts of the process for other applications. For example, silica-rich residues could be used in alkali-activated materials such as concrete, while part of the cellulose stream could be converted into biofuels. A bleaching step should also be investigated to improve the optical properties of the fibres, since previous results show that color differences are more significant than brightness differences compared to the reference pulp.

Further development of the process could also be linked to industrial fibre production methods such as those used by TreeToTextile. It would be relevant to investigate how the produced pulp can be adapted to this type of spinning process.

Process optimisation could also include studying cooking time and temperature. Previous research has shown that lower temperatures can sometimes be used while still achieving good delignification, which may reduce energy consumption.

From a wider perspective, a life cycle assessment (LCA) would be useful to compare the environmental impact of annual plants and wood-based materials. This would help to understand whether non-wood fibres are environmentally beneficial at larger scale. In this work, only wheat straw was studied, so it would also be useful to test other annual plants to see how results change between different feedstocks. A related study could also include seasonal variation and differences in cultivation conditions, since these may affect fibre quality and process performance.

Finally, differential scanning calorimetry (DSC) measurements could be used to better understand the material structure, for example to gain information about porosity and thermal behaviour, which may be important for further processing and final material properties.

Bibliography

- [1] European Parliament. *Update of the Waste Framework Directive: Textile and food waste*. 2025. URL: [https://www.europarl.europa.eu/thinktank/en/document/EPRS_BRI\(2023\)757572](https://www.europarl.europa.eu/thinktank/en/document/EPRS_BRI(2023)757572).
- [2] European Environment Agency. *Textiles*. 2026. URL: <https://www.eea.europa.eu/en/topics/in-depth/textiles>.
- [3] GENeco. *Fast Fashion and Its Impacts*. 2026. URL: <https://www.geneco.uk.com/news/fast-fashion-and-its-impacts>.
- [4] Elisabet Quintana, Cristina Valls, and M. Blanca Roncero. “Dissolving-grade pulp: a sustainable source for fiber production”. In: *Wood Science and Technology* 58 (Jan. 2024), pp. 23–85. ISSN: 14325225. DOI: 10.1007/s00226-023-01519-w.
- [5] Zhong Liu, Huimei Wang, and Lanfeng Hui. “Pulping and Papermaking of Non-Wood Fibers”. In: *Pulp and Paper Processing*. InTech, Oct. 2018. DOI: 10.5772/intechopen.79017.
- [6] Pratima Bajpai. *Biermann’s Handbook of Pulp and Paper: Raw Material and Pulp Making: Volume 1, Third Edition*. Vol. 1. Elsevier, Jan. 2018, pp. 1–647. DOI: 10.1016/C2017-0-00513-X.
- [7] Mingxing Sun, Yutao Wang, and Lei Shi. “Environmental performance of straw-based pulp making: A life cycle perspective”. In: *Science of the Total Environment* 616-617 (Mar. 2018), pp. 753–762. ISSN: 18791026. DOI: 10.1016/j.scitotenv.2017.10.250.
- [8] Joanna Wojtasz et al. “Producing dissolving pulp from agricultural waste”. In: *RSC Sustainability* 3 (Mar. 2025), pp. 2210–2220. ISSN: 27538125. DOI: 10.1039/d4su00534a.
- [9] Mohamed Said et al. “Wheat Straw: Phytochemical and Pharmacological Aspects”. In: *Importance of Plant Based Byproducts: Nutritional and Functional Properties*. Springer Nature Switzerland, 2026, pp. 263–288. DOI: 10.1007/978-3-032-03503-5_{_}10.
- [10] Seyed Hamidreza Ghaffar. “Wheat straw biorefinery for agricultural waste valorisation”. In: *Green Materials* 8 (Nov. 2019), pp. 60–67. ISSN: 20491239. DOI: 10.1680/jgrma.19.00048.
- [11] TreeToTextile. *Our technology*. URL: <https://treetotextile.com/our-technology/>.
- [12] Herbert Sixta. *Handbook of Pulp*. Vol. 1-2. John Wiley and Sons, Jan. 2008, pp. 1–1352. DOI: 10.1002/9783527619887.
- [13] Martin Kihlman. *Dissolution of cellulose for textile fibre applications*. Tech. rep. Karlstad: Karlstad University, 2012.
- [14] Liming Zhang et al. “Comparison of lignin distribution, structure, and morphology in wheat straw and wood”. In: *Industrial Crops and Products* 187 (Nov. 2022). ISSN: 09266690. DOI: 10.1016/j.indcrop.2022.115432.

- [15] Ruigang Liu, Hui Yu, and Yong Huang. “Structure and morphology of cellulose in wheat straw”. In: *Cellulose* 12.2005 (2005), pp. 25–34. DOI: 10.1007/s10570-004-0955-8.
- [16] Björn Lindman, Gunnar Karlström, and Lars Stigsson. “On the mechanism of dissolution of cellulose”. In: *Journal of Molecular Liquids* 156 (Sept. 2010), pp. 76–81. ISSN: 01677322. DOI: 10.1016/j.molliq.2010.04.016.
- [17] Alfred D. French. “Glucose, not cellobiose, is the repeating unit of cellulose and why that is important”. In: *Cellulose* 24 (Nov. 2017), pp. 4605–4609. ISSN: 1572882X. DOI: 10.1007/s10570-017-1450-3.
- [18] Eero Sjöström. *Wood Chemistry Fundamentals and Applications*. English. Second. Elsevier, 1993. ISBN: 978-0-08-092589-9. DOI: 10.1016/C2009-0-03289-9.
- [19] Surachet Imlimthan et al. “Introduction to lignocellulosic materials”. In: *Lignin-based Materials for Biomedical Applications: Preparation, Characterization, and Implementation*. Elsevier, Jan. 2021, pp. 1–34. DOI: 10.1016/B978-0-12-820303-3.00010-2.
- [20] Run Cang Sun, X. F. Sun, and J. Tomkinson. “Hemicelluloses and their derivatives”. In: *ACS Symposium Series* 864 (2004), pp. 2–22. ISSN: 00976156. DOI: 10.1021/bk-2004-0864.ch001.
- [21] Charles M. Buchanan et al. “Preparation and characterization of arabinoxylan esters and arabinoxylan ester/cellulose ester polymer blends”. In: *Carbohydrate Polymers* 52 (June 2003), pp. 345–357. ISSN: 01448617. DOI: 10.1016/S0144-8617(02)00290-4.
- [22] Seyed Hamidreza Ghaffar and Mizi Fan. “Structural analysis for lignin characteristics in biomass straw”. In: *Biomass and Bioenergy* 57 (Oct. 2013), pp. 264–279. ISSN: 09619534. DOI: 10.1016/j.biombioe.2013.07.015.
- [23] Maja Lindblad. *Alkaline wet oxidation of biorefinery lignin from wheat straw*. Tech. rep. Lund: Lund University, 2021. URL: <https://lup.lub.lu.se/student-papers/search/publication/9066729>.
- [24] Dilling. P and Sarjeant. T. P. *Reduction of lignin color*. 1982.
- [25] Antti Koistinen, Tapani Vuorinen, and Thaddeus Maloney. “The effect of alkaline pre-treatment on cellulose pulp fiber dissolution”. In: *Carbohydrate Polymer Technologies and Applications* 11 (Sept. 2025). ISSN: 26668939. DOI: 10.1016/j.carpta.2025.100978.
- [26] Chunxia Chen et al. “Cellulose (dissolving pulp) manufacturing processes and properties: A mini-review”. In: *BioResources* 11.2 (Mar. 2016), pp. 5553–5564. ISSN: 19302126. DOI: 10.15376/biores.11.2.Chen.
- [27] Xiaoya Jiang et al. “A review on raw materials, commercial production and properties of lyocell fiber”. In: *Journal of Bioresources and Bioproducts* 5 (Feb. 2020), pp. 16–25. ISSN: 23699698. DOI: 10.1016/j.jobab.2020.03.002.
- [28] Raimo Alén. “Pulp Mills and Wood-Based Biorefineries”. In: *Industrial Biorefineries and White Biotechnology*. Elsevier, May 2015, pp. 91–126. DOI: 10.1016/B978-0-444-63453-5.00003-3.
- [29] Tatiana Budtova and Patrick Navard. “Cellulose in NaOH-water based solvents: a review Cellulose in NaOH-water based solvents : a review”. In: *Cellulose* 23.2016 (2015), pp. 5–55. DOI: 10.1007/s10570-015-0779-8.
- [30] B Lönnberg, M El-Sakhawy, and T Hultholm. “Ethanol pulping of pretreated non-wood fibre materials”. In: *The Chemistry and Processing of Wood and Plant Fibrous Material*. Elsevier, 1996, pp. 99–109. DOI: 10.1533/9781845698690.99.

- [31] Ziyuan Zhou et al. “Lignocellulosic biomass to biofuels and biochemicals: A comprehensive review with a focus on ethanol organosolv pretreatment technology”. In: *Biotechnology and Bioengineering* 115 (Nov. 2018), pp. 2683–2702. ISSN: 10970290. DOI: 10.1002/bit.26788.
- [32] Weiping Deng et al. “Catalytic conversion of lignocellulosic biomass into chemicals and fuels”. In: *Green Energy and Environment* 8 (Feb. 2023), pp. 10–114. ISSN: 24680257. DOI: 10.1016/j.gee.2022.07.003.
- [33] Huan Chen et al. “Mechanism insight into photocatalytic conversion of lignin for valuable chemicals and fuels production: A state-of-the-art review”. In: *Renewable and Sustainable Energy Reviews* 147 (Sept. 2021). ISSN: 18790690. DOI: 10.1016/j.rser.2021.111217.
- [34] Akash Mamon Sarkar et al. “Dissolving pulp from non-wood plants by prehydrolysis potassium hydroxide process”. In: *Cellulose Chemistry and Technology* 55 (2021), pp. 117–124. ISSN: 05769787.
- [35] Feng Liu et al. “Synergistic utilization of cold caustic extraction and deep eutectic solvent for the production of dissolving pulp from corn stalks”. In: *Biomass and Bioenergy* 184 (May 2024). ISSN: 18732909. DOI: 10.1016/j.biombioe.2024.107184.
- [36] Gloria I. Ngene, Jean Claude Roux, and Dominique Lachenal. “Influence of Hollander Beater Refining on Xylan Extraction from Hardwood Paper Pulp by Cold Caustic Extraction and Xylanase Treatment”. In: *BioResources* 17 (2022), pp. 908–921. ISSN: 19302126. DOI: 10.15376/biores.17.1.908-921.
- [37] Antti Koistinen et al. “Effect of pulp prehydrolysis conditions on dissolution and regenerated cellulose pore structure”. In: *Cellulose* 30 (Mar. 2023), pp. 2827–2840. ISSN: 1572882X. DOI: 10.1007/s10570-023-05050-w.
- [38] J. M.B. Fernandes Diniz, M. H. Gil, and J. A.A.M. Castro. “Hornification - Its origin and interpretation in wood pulps”. In: *Wood Science and Technology* 37 (Apr. 2004), pp. 489–494. ISSN: 00437719. DOI: 10.1007/s00226-003-0216-2.
- [39] Thaddeus Maloney et al. “Deaggregation of cellulose microfibrils and its effect on bound water”. In: *Carbohydrate Polymers* 319 (Nov. 2023). ISSN: 01448617. DOI: 10.1016/j.carbpol.2023.121166.
- [40] Håkan Wennerström and Björn Lindman. “Dissolution of cellulose in alkali: A competition between ionization and hydrophobic interactions.” In: *Journal of Molecular Liquids* 436 (2025). ISSN: 01677322. DOI: 10.1016/j.molliq.2025.128169.
- [41] Runcang Sun, J. Mark Lawther, and W. B. Banks. “Influence of alkaline pretreatments on the cell wall components of wheat straw”. In: *Industrial Crops and Products* 4 (1995), pp. 127–145. ISSN: 09266690. DOI: 10.1016/0926-6690(95)00025-8.
- [42] Weiqing Liu, Tatiana Budtova, and Patrick Navard. “Influence of ZnO on the properties of dilute and semi-dilute cellulose-NaOH-water solutions”. In: *Cellulose* 18 (Aug. 2011), pp. 911–920. ISSN: 09690239. DOI: 10.1007/s10570-011-9552-9.
- [43] Johannes Schindelin et al. “Fiji: An open-source platform for biological-image analysis”. In: *Nature Methods* 9 (July 2012), pp. 676–682. ISSN: 15487091. DOI: 10.1038/nmeth.2019.
- [44] Emma Åkesson and Emma Skotte. *Organosolv using Wheat Straw - Dissolving Pulp Production and Process Simulation*. Tech. rep. Gothenburg: Chalmers, 2023. URL: <https://odr.chalmers.se/items/f15104c9-39b4-4ad6-bdda-fe133316e518>.

- [45] Leandro Cid Gomes et al. “Green Biorefinery Side Stream as a Source of Chlorophyll Pigments, Lignin, and Cellulose for Textile Fibers”. In: *ACS Sustainable Chemistry and Engineering* 13 (Oct. 2025), pp. 16946–16957. ISSN: 21680485. DOI: 10.1021/acssuschemeng.5c06653.

A. Appendix

A.1 Equations for pretreatment and pulping process

A.1.1 Dry content

$$d = \frac{m_{\text{dry pulp}}}{m_{\text{wet pulp}}} \quad (\text{A.1})$$

A.1.2 Mass yield

$$Y_m = \frac{m_{\text{after}}}{m_{\text{dry, initial}}} \quad (\text{A.2})$$

A.1.3 Actual NaOH concentration

$$C_{\text{NaOH,actual}} = \frac{m_{\text{NaOH}}}{m_{\text{NaOH}} + m_{\text{water}} + m_{\text{wet}}(1 - d)} \quad (\text{A.3})$$

A.1.4 Actual L/S ratio

$$L/S_{\text{actual}} = \frac{m_{\text{NaOH}} + m_{\text{water}} + m_{\text{wet}}(1 - d)}{m_{\text{wet}}d} \quad (\text{A.4})$$

A.1.5 Water to add

$$m_{\text{water,add}} = (L/S \cdot m_{\text{dry pulp}}) - (m_{\text{liquid,total}} \cdot C_{\text{NaOH}}) - m_{\text{wet pulp}}(1 - d) \quad (\text{A.5})$$

A.2 Compositional data of samples

Table A.1: Composition of wheat straw after pretreatment.

Pretreatment	EA (g NaOH/100 g dry)	Ara	Rha	Gal	Glu	Xyl	Man	Klason	ASL	Sum
50% EtOH	0.332	0.55	-	-	68.61	13.30	-	3.60	0.69	86.75
50% EtOH / 0.15% acid	0.332	0.12	-	-	74.81	7.91	-	6.30	0.59	89.72
50% EtOH / 0.15% acid	0.48	0.06	-	-	81.14	6.14	0.56	6.27	0.66	94.83
50% EtOH	0.48	0.28	-	-	83.09	11.44	0.78	6.83	0.45	102.87
65% EtOH	0.48	0.22	-	-	88.42	10.10	0.68	1.58	0.74	101.72
50% EtOH / 0.10% acid	0.48	0.10	-	-	91.57	6.23	0.60	2.03	0.72	101.25
Hot water / 0.1%HCl	0.56	0.30	-	-	89.20	10.30	0.30	2.70	-	102.80
65% EtOH	0.72	0.08	-	-	94.38	4.06	0.69	1.83	0.72	101.76
50% EtOH / 0.10% acid	0.72	0.06	-	-	89.89	3.22	0.64	1.25	0.61	95.67
50% EtOH / 0.2% acid	0.96	0.06	-	-	95.45	2.15	0.67	9.87	0.86	109.06
50% EtOH	0.96	0.05	-	-	84.72	1.73	0.30	7.70	0.35	94.84

Table A.2: Composition of extracted wheat straw samples. With pretreatment condition of 50% ethanol/water

EA (g NaOH/100 g dry)	Ara	Rha	Gal	Glu	Xyl	Man	Klason	ASL	Sum
0.48	0.17	-	-	85.64	8.51	0.65	5.26	0.67	100.9
0.96	0.05	-	-	92.36	1.65	0.64	3.56	0.64	98.90

Table A.3: Composition of untreated wheat straw

Ara	Rha	Gal	Glu	Xyl	Man	Klason	ASL	Sum
1.77	-	-	42.31	22.89	-	19.94	2.97	89.88

Table A.4: Composition of grass sample after pretreatment

Ara	Rha	Gal	Glu	Xyl	Man	Klason	ASL	Sum
0.21	-	-	85.62	8.17	0.50	2.29	0.83	97.62

A.3 Brightness of samples

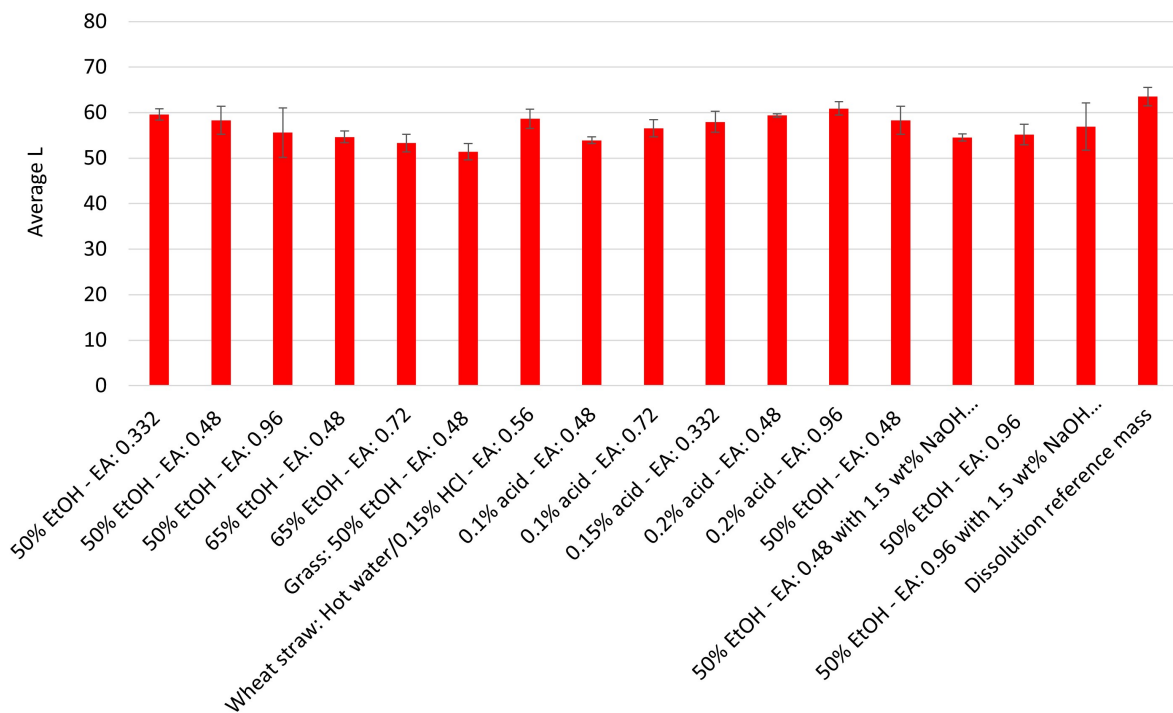


Figure A.1: Average L-value between cellulose pulps and reference

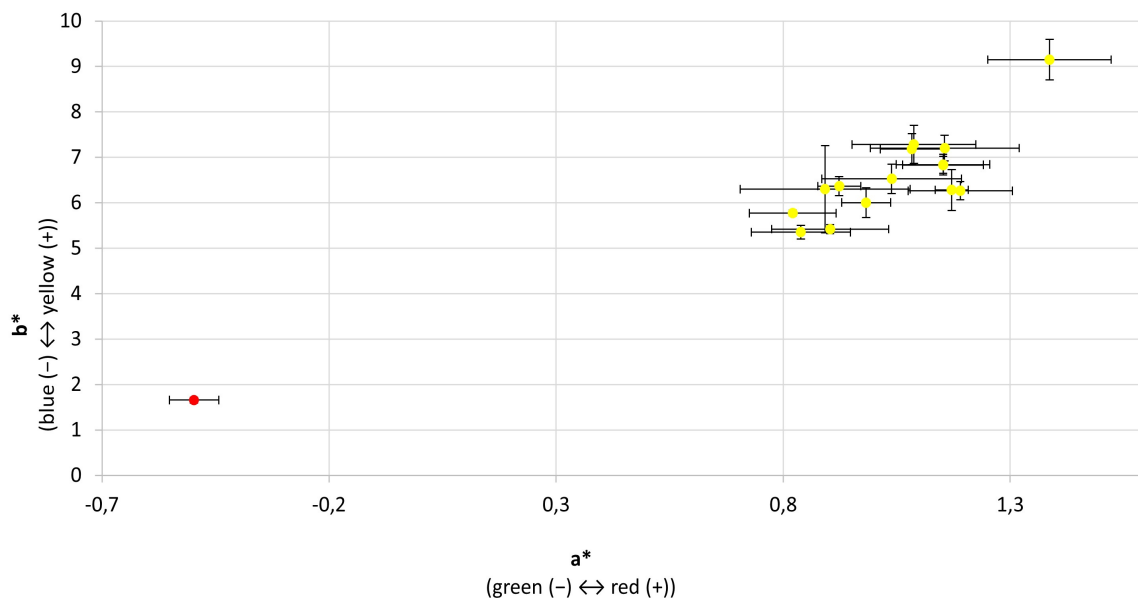


Figure A.2: Colour distribution of cellulose samples in the A and B colour space. The red marker indicates the dissolution reference sample and the yellow marker indicate all the samples.

A.4 EMIMAc dissolution



(a) EMIMAc dissolution bright field

(b) EMIMAc dissolution polarized

Figure A.3: EMIMAc dissolution of the 50% ethanol sample with $EA = 0.48$.

A.5 Equations - Intrinsic viscosity

The viscosity ratio, $\eta_{\text{ratio}} = \eta/\eta_0$, was calculated using

$$\eta_{\text{ratio}} = h \cdot t$$

where $h = 0.102$ and t is the efflux time in seconds. Using the measured viscosity ratio, the corresponding value for $[\eta] \times \rho$ was obtained from a table.

The mass concentration of the solution was calculated as

$$c = \frac{m \cdot DM}{25 + (1 - DM)m + V_w}$$

The limiting viscosity number, $[\eta]$, was calculated using

$$[\eta] = \frac{[\eta] \times \rho}{\rho} = ([\eta] \times \rho) \frac{25 + (1 - DM)m + V_w}{m \cdot DM}$$

where $[\eta] \times \rho$ is the value obtained from a table corresponding to the measured viscosity ratio. The limiting viscosity number is expressed in millilitres per gram.

DEPARTMENT OF CHEMISTRY AND CHEMICAL ENGINEERING
CHALMERS UNIVERSITY OF TECHNOLOGY

Gothenburg, Sweden

www.chalmers.se



CHALMERS
UNIVERSITY OF TECHNOLOGY